L.D. van der Pijl

Identification of muscles (un)loading the UCL during baseball pitching

TU Delft

Identification of muscles (un)loading the UCL during baseball pitching

By

L.D. van der Pijl

in partial fulfilment of the requirements for the degree of

Master of Science
In
Biomedical Engineering

at the Delft University of Technology.

Daily supervisor:	B. van Trigt, PhD candidate
Supervisor:	Prof. dr. F.C.T. van der Helm

.

TU Delft

Abbreviations

Abbreviation	Meaning
ANC	Anconeus
BIC	Biceps Brachii
BRA	Brachialis
BRD	Brachioradialis
CoP	Center of Pressure
DoF	Degrees of Freedom
ECRB	Extensor Carpi Radialis Brevis
ECRL	Extensor Carpi Radialis Longus
ECU	Extensor Carpi Ulnaris
EDC	Extensor Digitorum Communis
EFE	Elbow Flexion-Extension
EMG	Electromyography
EVV	Elbow Varus-Valgus
FCR	Flexor Carpi Radialis
FCU	Flexor Carpi Ulnaris
FDS	Flexor Digitorum Superficialis
MER	Maximum External Rotation
MEV	Maximum External Valgus-moment
MLB	Major League Baseball
PRO	Pronator Teres
PS	Pronation-Supination
SD	Standard Deviation
SO	Static Optimization
SUP	Supinator
TDSEM	Thoracoscapular Delft Shoulder and Elbow Model
TRI	Triceps Brachii
UCL	Ulnar Collateral Ligament

Contents

Abstract

Injury to the Ulnar Collateral Ligament (UCL) is common among baseball pitchers, due to high external valgus torques applied around the elbow during pitching. Literature shows that elbow muscles and the osseous articulation can lower the load imposed to the UCL by countering the external valgus moment. As the contribution of the individual elbow muscles and the osseous articulation to the UCL load during pitching remains unclear, this study aims to identify the muscles capable of (un)loading the UCL during baseball pitching. Muscle-driven simulations for ten baseball pitches were generated using a musculoskeletal (MSK) model of the upper extremity. The simulations were run twice: ones without any constrictions to the model and ones with the wrist motion locked. The flexor digitorum superficialis (FDS) was identified as biggest contributors to the internal muscle moment during the wrist-included simulations. The external valgus torque was 10% countered by the elbow muscles, 59% by the osseous articulation and 31% by the UCL. The UCL had to resist a moment of 25.6 Nm. During the wrist-excluded simulations, the flexor carpi radialis (FCR) and was identified as biggest contributors to the internal muscle moment. The external valgus torque was 10% countered by the elbow muscles, 42% by the osseous articulation and 48% by the UCL, resulting in a UCL moment of 39.4 Nm. Further research should focus on the influence of wrist and finger motion on UCL load and concentrate more on the osseous articulation as main elbow stabilizer during pitching.

1. Introduction

Injury to the Ulnar Collateral Ligament (UCL) is common among baseball pitchers (Anz et al., 2010). Cases of UCL injuries increased over the past decades. The prevalence of UCL reconstruction in professional baseball players has increased by 3% from 2012 to 2018 (from 10 to 13%) (Leland et al., 2019). Between 2010 and 2015, 113 UCL reconstructions had been conducted on Major League Baseball (MLB) pitchers (Conte et al., 2016). These injuries are associated with substantial recovery and costs (Meldau et al., 2020). MLB pitchers require a mean time of 17.8 months to return to their prior level of competition (Conte et al., 2016). The cost of recovery was on average 1.9 million dollars per player from 2004 to 2014 (Meldau et al., 2020). Thus, the development of strategies for UCL injury prevention is crucial.

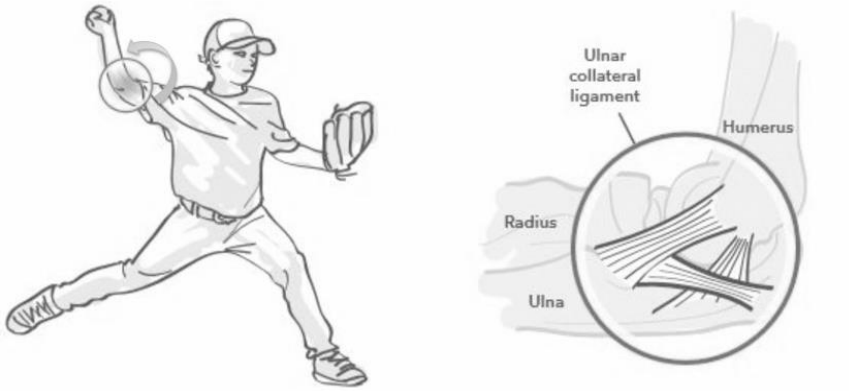

Fig.1. Illustration of the external valgus motion of the elbow and the UCL crossing the elbow joint (Ahmad, 2017).

During pitching motions, an external torque is applied around the elbow (Fig.1.). This external torque can be divided into two rotational axes: the elbow flexion-extension axis and the varus-valgus axis. (Fig. 2.) The torque around the flexion-extension axis causes the elbow to move during the pitch. The torque around the varus-valgus axis causes a valgus motion which leads to instability of the elbow joint and tension to the UCL (Fig. 2.). This external valgus torque needs to be countered by an internal varus torque to maintain the stability of the elbow joint during pitching. The UCL is the primary stabilizer of the elbow joint by resisting external valgus motion (Lee & Rosenwasser, 1999). Fleisig et al. (1995) reported that the external valgus torque acting on the elbow during a pitch for professional baseball players is 60-120 Nm. This torque is larger than the ultimate torque the UCL can resist, namely 30 Nm (Ahmad et al., 2003; Anz et al., 2010; McGraw et al., 2012). This puts the UCL at risk of injury. However, not every time a baseball pitcher throws a ball, the UCL gets injured. This suggests that other mechanisms and/or structures, next to the UCL, contribute to valgus stability as well.

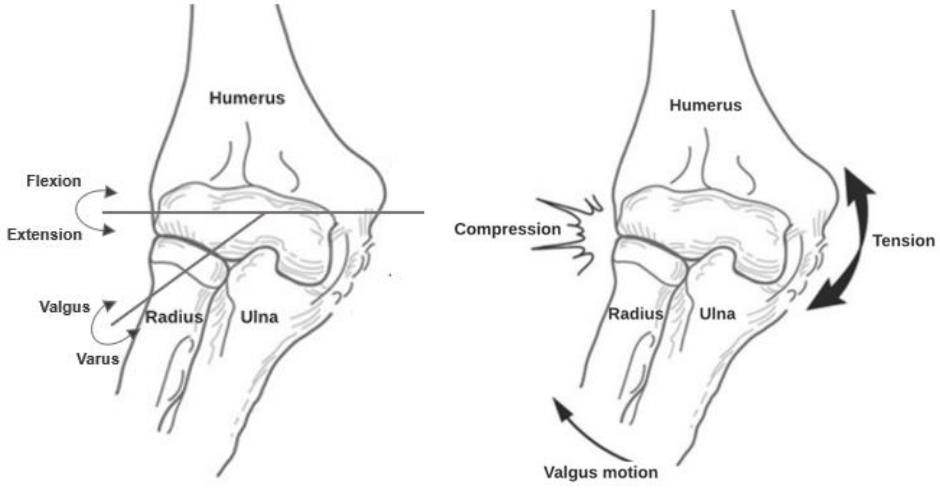

Fig.2. Illustration of the elbow flexion-extension axis and the varus-valgus axis (left). Illustration of the valgus motion causing tension on the UCL (right). Adjusted from O'Connell & Field, 2020.

Several in vitro studies have investigated the role of elbow muscles in reducing tension on the UCL by increasing tension in the elbow muscles of a cadaveric model. The flexor carpi ulnaris (FCU), the pronator teres (PRO), flexor digitorum superficialis (FDS), and the flexor carpi radialis (FCR) were reported to lessen the UCL tension (Davidson et al., 1995; Lin et al., 2007; Seiber et al., 2009; Udall et al., 2009). Tension of the supinator (SUP), brachioradialis (BRD), extensor carpi radialis longus (ECRB) and extensor carpi radialis brevis (ECRL), extensor digitorum communis (EDC) and extensor carpi ulnaris (ECU) was reported to induce valgus motion of the elbow (Lin et al., 2007; Seiber et al., 2009). These results indicate that the elbow muscles can have a direct effect on the UCL load, by generating an internal varus of valgus toque. In addition, Morrey et al. (1991) and Seiber et al. (2009) reported that loading of the biceps (BIC) and triceps brachii (TRI) in a cadaveric arm model can increase the joint compression force of the elbow joint and resists external valgus load in this way. Ferreira et al. (2010) conducted a similar experiment by loading the BIC, TRI and brachialis (BRA) of a cadaveric arm model and measuring the force exposed to the UCL simultaneously. They concluded that muscle activity of the BIC, TRI and BRA offloads the UCL by increasing the joint compression force and decreasing the joint space. These results indicate co-contraction of the elbow flexor and extensor muscles as a possible contributor to counteracting the external valgus torque. Although these studies show the potential role of the elbow muscles in (un)loading the UCL, these experiments were conducted on cadaveric models and static forces were manually applied to the muscles. It remains unclear whether the elbow muscles are active in the same manner during dynamic motions like pitching.

Unfortunately, it is currently not possible to directly measure individual muscle and joint forces during pitching due to the difficulty of instrumenting living tissues and ethical considerations. Common indirect measurements include surface electromyography (EMG) (Frost et al., 2010). Surface EMG provides a good insight into muscle activation levels during dynamic tasks. Van Trigt et al. (2021) used EMG to determine which muscles crossing the elbow are active during pitching. The flexor pronator mass, which consists of the FDS, FCR and FCU, PRO, TRI, BIC, and the extensor supinator mass, which consists of the SUP, BRD, ECRB, ECRL, EDC and ECU, and anconeus (ANC) were under investigation. At the moment of maximal external rotation (MER), when the external valgus torque reaches its maximum, all muscles showed moderate activity. However, EMG data still provides insufficient information regarding muscle force magnitudes, especially during dynamic tasks (Schellenberg et al., 2015). Musculoskeletal models (MSK) are able to provide a link between externally measured data and internal forces and moments. MSK models can therefore serve as a non-invasive research tool to investigate the activation of individual muscles on one or multiple joints, calculate joint forces, examine ligament function, and investigate joint stability over a wide range of motion (Gonzales et al., 1996). The development of software tools for MSK modelling has expanded the use of MSK models. These software tools allow users to create and share models easily (Correa, 2016; Valente, 2017).

Buffi et al. (2015) were the first ones who tried to predict the contribution of muscles, the UCL and the elbow joint to the internal varus moment during pitching motions using an MSK model. The MSK model was a right upper limb model and included six degrees of freedom (DoF); adduction, flexion, and rotation at the shoulder, flexion and varus at the elbow, and pronation at the forearm. Muscles included in the model were: the ANC, BIC, TRI, BRA, FCR, FCU, FDS and PRO. Buffi et al. (2015) developed a simulation framework that can reveal which muscles have the biggest moment-generating capacities during baseball pitching. They found that increasing the outputs of muscle-tendon units also increased the joint compression force and decreased the UCL load. The medial elbow muscles were all active during the simulations and contributed to the total internal varus moment. At the moment of peak valgus loading, the TRI generated large internal varus moments. The highest internal varus moments were generated by the FDS and occurred later in the motion. These findings are consistent with the results of the cadaveric studies (Morrey et al. 1991; Davidson et al., 1995; Lin et al., 2007; Seiber et al., 2009; Udall et al., 2009). However, the lateral elbow muscles were not included in this study, so the influence of contraction of the lateral muscles on the joint stability remains unclear. In addition, the model used in this study only represents elbow-spanning muscles. However, it is reasonable to assume that shoulder- and wrist-spanning muscles influence joint reaction forces and ultimately joint stability. It is known that individual muscles not only act to accelerate the joint it spans, but also other joints. This is called dynamic coupling (Zajac, 1993; Zajac and Gordon, 1989). Besides this, the wrist joint and the joints in the hand of the model were fixed. Although, kinematic data of these joint show were small motions, this could influence the activation patterns of the muscles and eventually the moments they generate.

Summarizing, research showed that an external valgus moment placed on the elbow not only gets countered by the UCL but also by muscles crossing the elbow joint and the osseous articulation. Forearm flexor muscles are able to generate internal varus moments and can therefore counter the external valgus moment directly (Morrey et al., 1981; Lin et al., 2007; Seiber et al., 2009; Udall et al., 2009; Buffi et al., 2015). Additionally, the interaction between the elbow muscles and the osteoarticular architecture can counter the external valgus moment indirectly by increasing the joint compression force and decreasing the joint space. This increases the contribution of the osseous articulation countering the external valgus moment (Morrey et al., 1991; Seiber et al., 2009; Ferreira et al., 2010; Van Trigt, 2021). It has been shown that the elbow muscles are active at MER and this suggests that muscles have a significant influence on regulating the elbow valgus load. However, the contribution of the individual elbow muscles and the osseous articulation to the UCL load during pitching remains unclear. Understanding how the individual elbow muscles contribute to the UCL load can lead to effective training of specific muscles and may alter the UCL load during pitching, protecting the UCL from injury (Maniar et al., 2022). In this way, UCL injuries among baseball players and the associated recovery time and costs can be reduced.

Therefore, this study aims to identify the muscles capable of (un)loading the UCL during baseball pitching. In more particular, (1) the elbow muscles capable of generating internal varus and/or valgus moments will be identified, (2) the forces and moments generated by the individual elbow muscles will be calculated, (3) the moment the UCL has to withstand will be quantified. Additionally, (4) the influence of wrist motion on muscle forces and the UCL load will be determined.

2. Methods

2.1. Musculoskeletal model

For this study, a previously developed and validated OpenSim MSK model of the upper extremity was applied and modified; the Thoracoscapular Delft Shoulder and Elbow Model (TDSEM) (De Vet, 2021). The TDSEM is a generic model containing 138 muscle elements crossing the shoulder and elbow. The model includes six rigid body segments, six joints and twelve DoF. The elbow joint contains the humeroulnar and the radioulnar joint. The humeroulnar joint is modelled as a hinge joint with one DoF, representing elbow flexion-extension. The radioulnar joint is modelled as a pivot joint with one DoF, representing forearm pronation-supination. An extra DoF was added to the humeroulnar joint representing elbow varus-valgus. In addition, a hinge joint was added between the radius and the hand representing wrist flexion extension. An overview of the DoFs of the elbow and wrist and the definitions of the joint angles used in this study are shown in Fig.3. The TDSEM was further developed by including forearm and hand muscles that cross the elbow, resulting in 150 muscle elements crossing the shoulder, elbow and wrist, see Appendix A. Morphological parameters of these muscles were obtained from Mirakhorlo et al. (2016). They constructed a complete anatomical data-set of the hand and wrist, including the intrinsic and extrinsic muscles through dissection and digitization of a right arm from a fresh-frozen cadaver (Female, 87 years old).

Muscle geometry is validated by comparing muscle moment arms of the model with muscle moment arms values taken from literature. This has been done for elbow flexion-extension (EFE), elbow varus-valgus (EVV) and pronation-supination (PS) moment arms. For validation of the EFE and PS moment arms, results from Ramsay et al. (2009) were taken for comparison. Ramsey et al. (2009) obtained muscle moment arms values from literature derived from both cadaveric measurements and MSK model calculations. With these muscle moment arms values, they created a range representing the maximum and minimum moment arm values cited from multiple sources at various elbow joint positions, for all elbow muscles. For validation of the EVV moment arms, results from An et al. (1981) were taken for comparison. An et al. (1981) performed dissections of six fresh upper extremity specimens to obtain the moment arms of each of the muscles along the upper arm and at the elbow joint in different positions. The maximum and minimum values of the moment arms of their results were taken for comparison. For the model used in this study, the muscle moment arm values were calculated over the entire range of motion for EFE, EVV and PS using OpenSim. The model's maximum and minimum moment arm values over the range of EFE, EVV and PS were taken. These values were compared with the results from Ramsay et al. (2009) and An et al. (1981) These results can be found in Appendix B. Based on these results, the muscle paths of 12 muscle

elements were then moved to represent the muscle geometry more accurate, see table 1. The final results can be found in Fig.4, 5 and 6. In Fig.7. the EFE and EVV moment arms are plotted against each other. The moment arms of every muscle were within or overlapped published data for EFE. For PS, the ECU together with the ECBR are outside the published literature range. For EVV, the ECU, FCR, FCU and FDS are outside the published literature range. The TRI and BIC both have moment arms in an opposite direction from those of the published literature range.

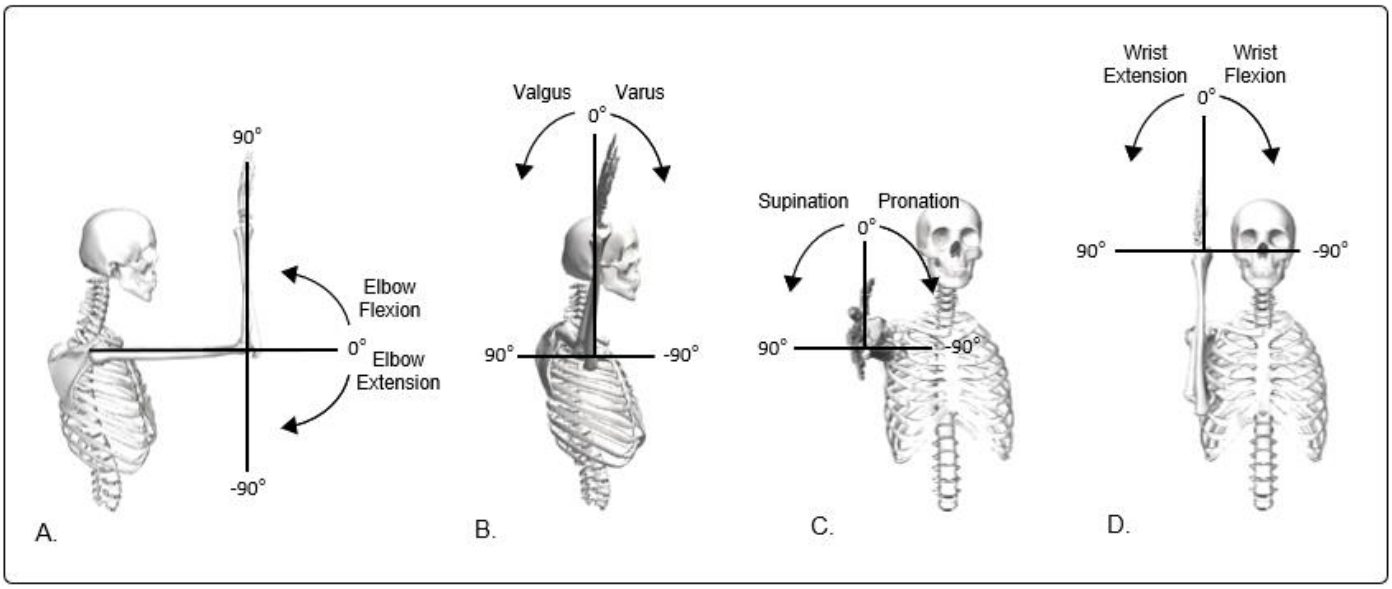

Fig.3. Definitions of the elbow angles used in this study; A. Elbow Flexion/Extension B. Varus/Valgus C. Pronation/Supination D. Wrist Flexion Extension.

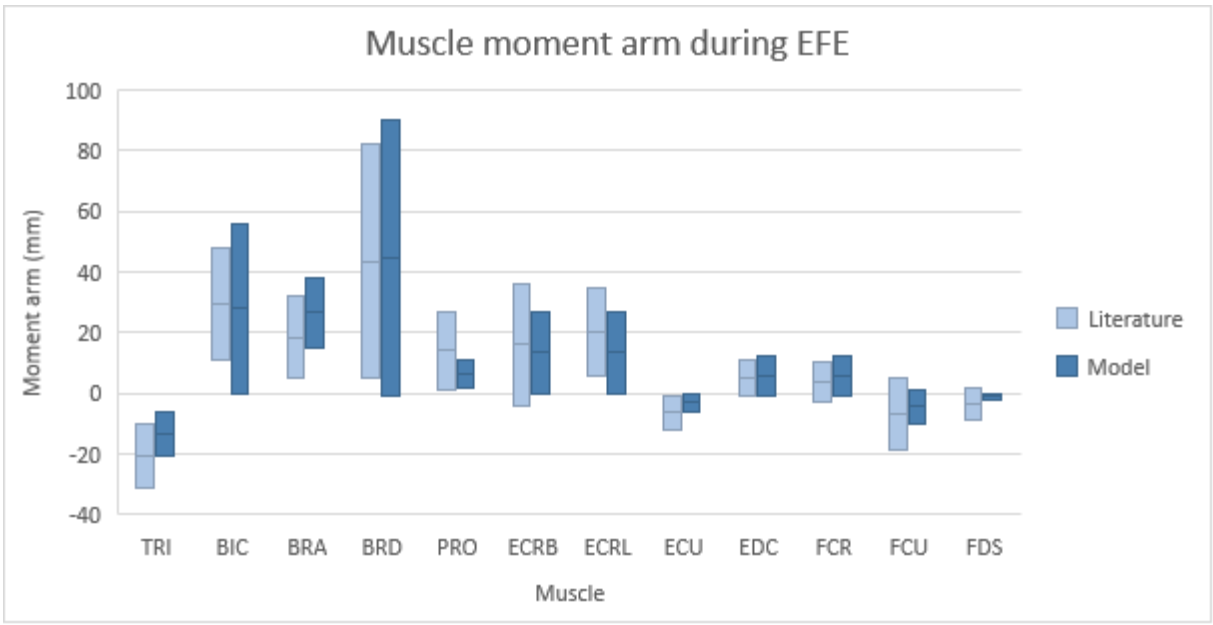

Fig.4. Comparison of literature moment arm range and model moment arm range during EFE. Positive and negative values correspond to elbow flexion and extension, respectively.

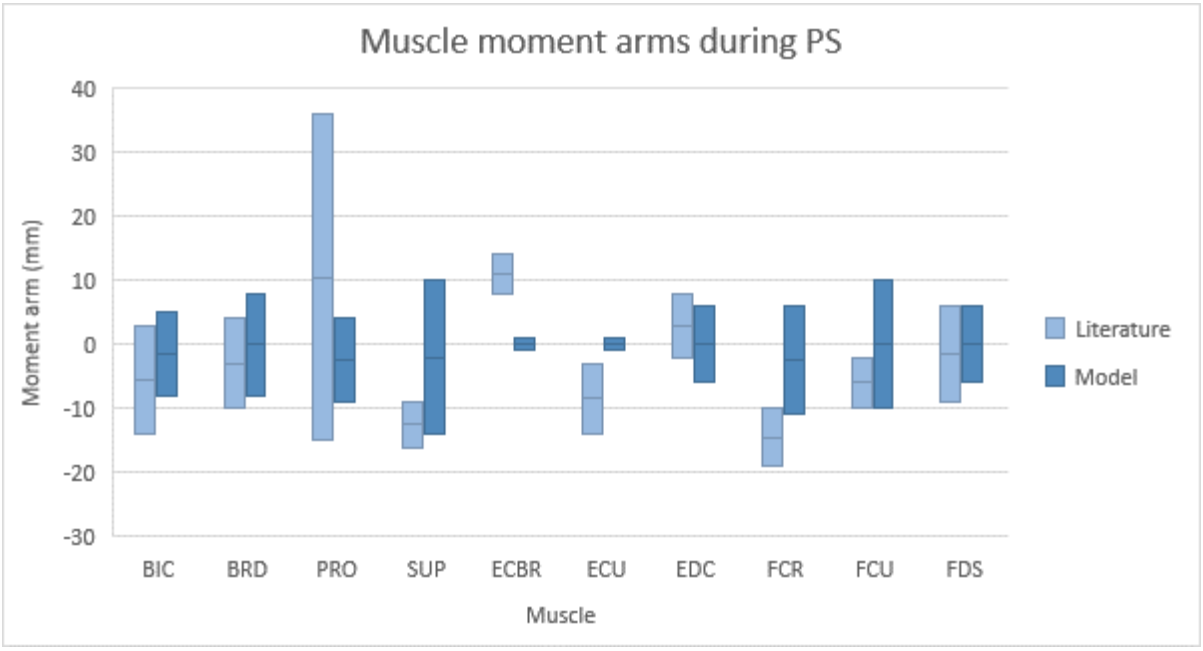

Fig.5. Comparison of literature moment arm range and model moment arm range during PS. Positive and negative values correspond to forearm pronation and supination, respectively.

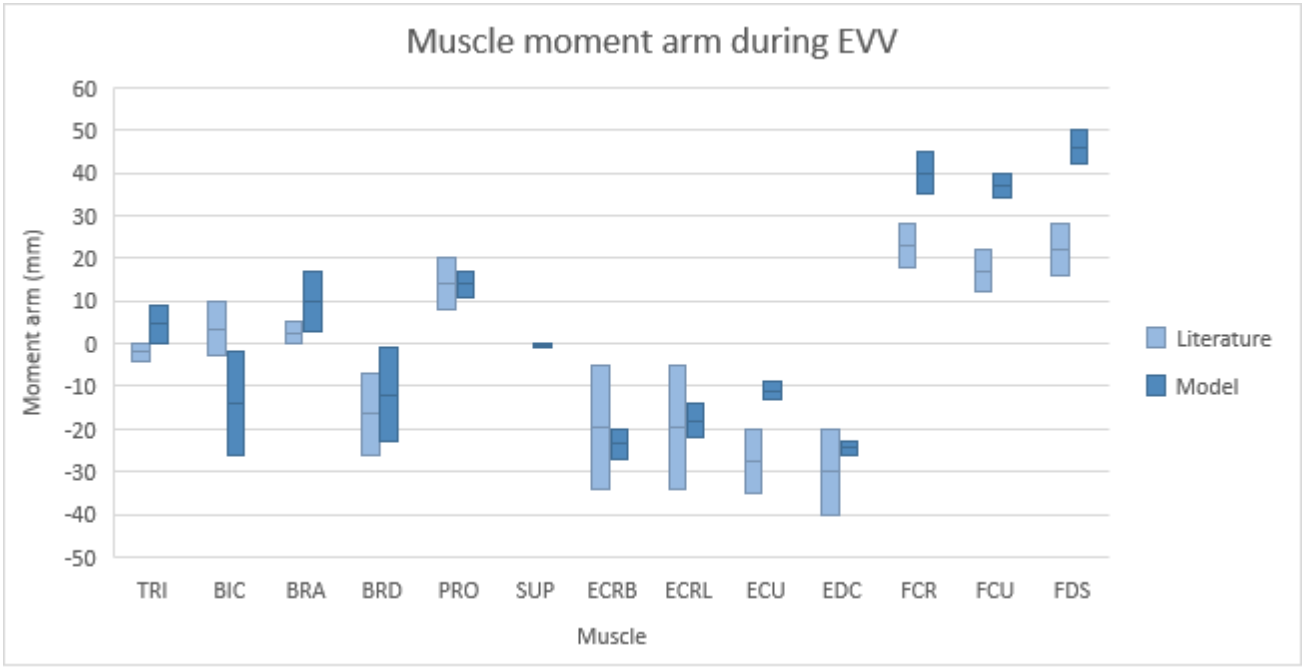

Fig.6. Comparison of literature moment arm range and model moment arm range during PS. Positive and negative values correspond to elbow varus and valgus, respectively.

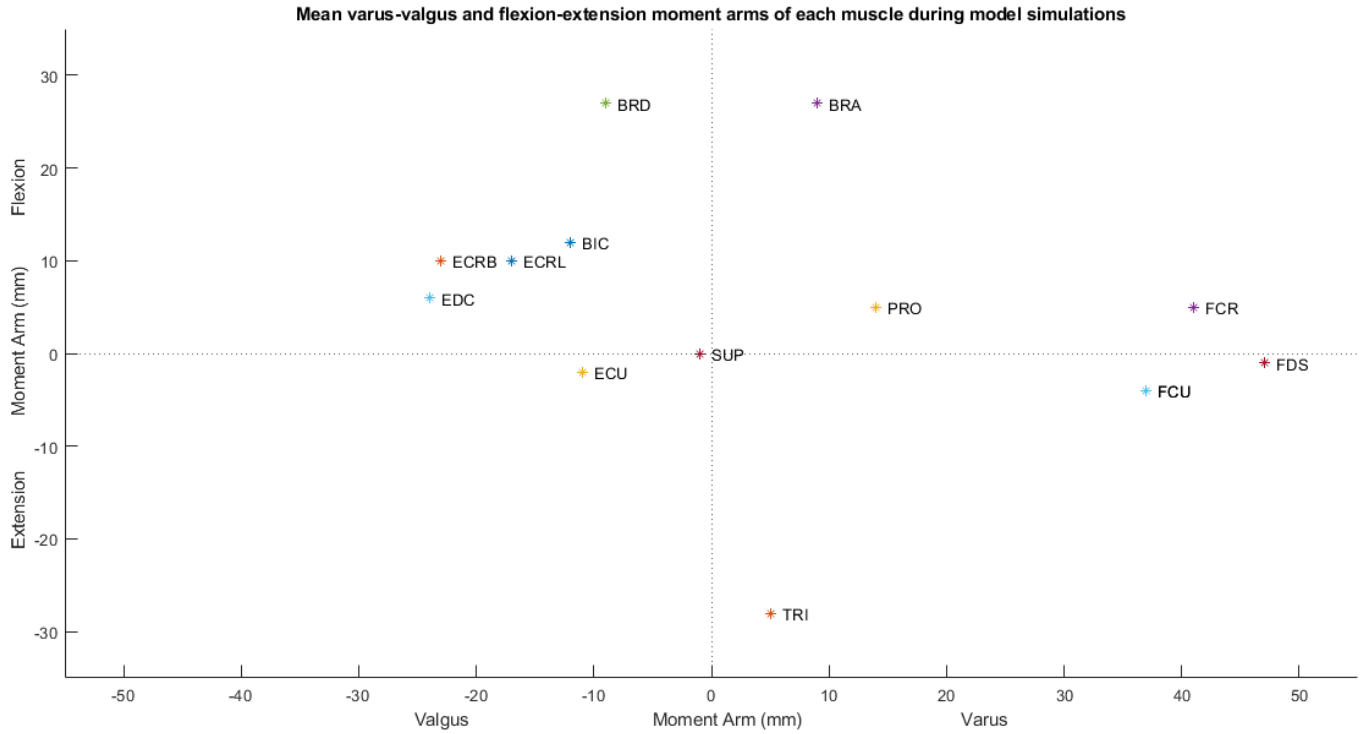

Fig.7. EFE and EVV moment arms plotted against each other.

Muscle-element	Original model Coordinates (x, y, z)	New model Coordinates (x, y, z)	Frame
Extensor Carpi Radius Brevis	(0.078, -0.274, -0.009) (0.061, -0.239, -0.03)	(0.024, -0.262, -0.009) (0.05, -0.239, -0.032)	Humerus Radius
Extensor Carpi Radialus Longus	(0.077, -0.28, -0.022) (0.053, -0.15, -0.025) (0.06, -0.217, -0.03)	(0.009, -0.261, 0.007) (0.028, -0.15, -0.032) (0.036, -0.217, -0.042)	Humerus Radius Radius
Extensor Carpi Ulnaris	(0.089, -0.289, -0.033) (0.062, -0.162, -0.003)	(0.019, 0, -0.001) (0.032, -0.072, -0.008)	Humerus Ulna
Extensor Digitorum 2	(0.061, -0.287, -0.023)	(0.03, -0.282, -0.002)	Humerus
Extensor Digitorum 3	(0.064, -0.288, -0.013)	(0.027, -0.28, -0.013)	Humerus
Extensor Digitorum 4	(0.066, -0.292, -0.001) (0.072, -0.26, -0.029)	(0.026, -0.284, -0.001) (0.044, -0.261, -0.034)	Humerus Ulna
Extensor Digitorum 5	(0.056, -0.026, -0.005)	(0.032, -0.027, -0.01)	Ulna
Flexor Digitorum Superficialis 2	(0.041, -0.286, -0.043) (0.038, -0.185, -0.049) (0.038, -0.201, -0.047)	(-0.021, -0.276. -0.006) (-0.02, -0.186, -0.06) (0.038, -0.201, -0.047)	Humerus Radius Radius
Flexor Digitorum Superficialis 3	(0.041, -0.286, -0.043) (0.048, -0.153, -0.042) (0.039, -0.216, -0.042)	(-0.022, -0.276, 0) (-0.015, -0.155, -0,054) (-0.01, -0.217, -0.052)	Humerus Radius Radius
Flexor Digitorum Superficialis 4	(0.032, -0.287, -0.2)	(-0.029, -0.274, -0.02)	Humerus
Flexor Digitorum Superficialis 5	(0.037, -0.283, -0.023) (0.018, -0.146, -0.021)	(-0.011, -0.273, -0.022) (-0.2, -0.147, -0.028)	Humerus Radius
Flexor Carpi Radialis	(0.012, -0.243, -0.004)	(-0.037, -0.278, -0.008)	Humerus
Flexor Carpi Ulnaris	(0.054, -0.274, -0.02) (0.031, -0.144, -0.002) (0.024, -0.2, -0.019)	(-0.004, -0.261, -0.02) (-0.028, -0.145, -0.014) (-0.003, -0.201, -0.025)	Humerus Radius Radius

Table 1. The modifications to muscle attachment points from Mirakhorlo et al. (2016).

2.2. Participants

A total of eleven male, right-handed pitchers with an average age of 22 (SD 4) years, body height of 1.91 (SD 0.05) m and body mass of 78.9 (SD 11) kg participated in this study. On average, they have 9 (SD 5) years of pitching experience. One pitcher is playing at the highest division in the Netherlands, the others at amateur level. The average ball speed of their throws was 66.8 (SD 4.1) mph.

2.3. Data acquisition

Motion analyses data were captured from 11 right-handed baseball players while pitching. Marker positions (Appendix.C) were recorded with a 120 Hz, 12 infrared camera 3D motion capture system (Flex 13 Optitrack, Natural Point). Per pitcher, 70-80 pitches were recorded. For each pitcher, the pitches with incomplete kinematic data, due to measure errors or lost markers, were filtered out. One pitcher got excluded from this study due to many errors in the data set. From the remaining data set, for every pitcher, the pitch with the highest ball speed was used for further analysis. Eventually, a total of ten pitches was analysed. Since the highest external valgus moment is known to occur in the period between foot contact and ball release (the arm cocking and acceleration phases), around the MER of the arm (Zheng et al., 2004), only these phases of the pitches were analysed (Fig.8.).

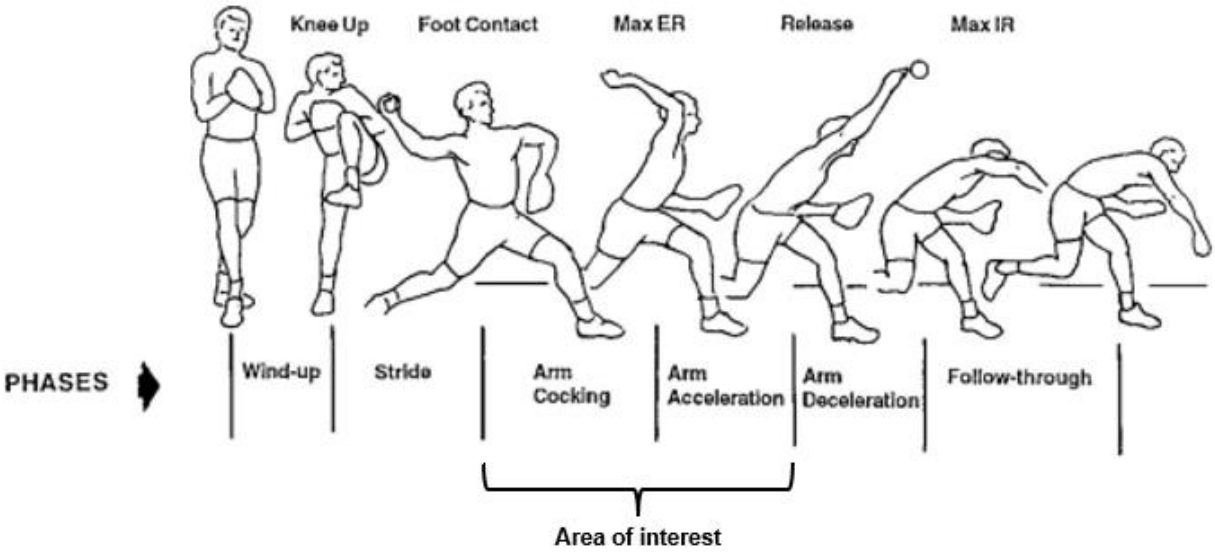

Fig.8. Different phases and events during the pitching motion (Stodden et al., 2001).

2.4. Model simulation

Marker position data were acquired in Motive 1.5.1 (NaturalPoint), converted to a C3D format and imported into Opensim (v4.1, http://simtk.org). The generic model was scaled, using the scaling tool provided in OpenSim, to match each participant's anthropometry based on static pose data, available from the experimental data set. Virtual markers were placed on the generic model with the same marker placements used in each subject. Once the model was scaled correctly, inverse kinematics were used to estimate the joint angles of the participant during the motion. A set of joint angles were computed by the inverse kinematics tool for each time step of the experimental motion data. The joint angles were computed using a weighted least squares optimization problem so that the marker error was minimized (Lu and O'Connor, 1999). The output joint angles were low-pass filtered with a cutoff frequency of 12 Hz. An inverse dynamics analysis was performed to calculate net joint torques from the motion kinematics so that the time instant of the external valgus torque and its magnitude could be determined. Muscle excitations were then

determined by using static optimization (SO). SO estimates muscle forces and activations by minimizing the sum of squared activations of each muscle (Thelen et al., 2003; Thelen and Anderson, 2006). Muscle activation data were lowpass-filtered with a cutoff frequency of 12 Hz. Residual- and reserve actuators were added to the model to enable the simulations to run. Residual actuators were added between the model and the ground to account for reaction forces. Reserve actuators were added to each of the model's joints to account for instances where the muscles cannot produce the needed force to perform the prescribed motion. From the results of each simulation, the individual muscle moments, the elbow joint compression force and the torque load on the UCL were calculated. The simulation steps are shown in Fig.9. For each pitch, the simulation was run two times. Ones without any constrictions to the model, wrist-included simulation, and ones with the motion of the wrist locked, wrist-excluded simulation. In total twenty simulations were run.

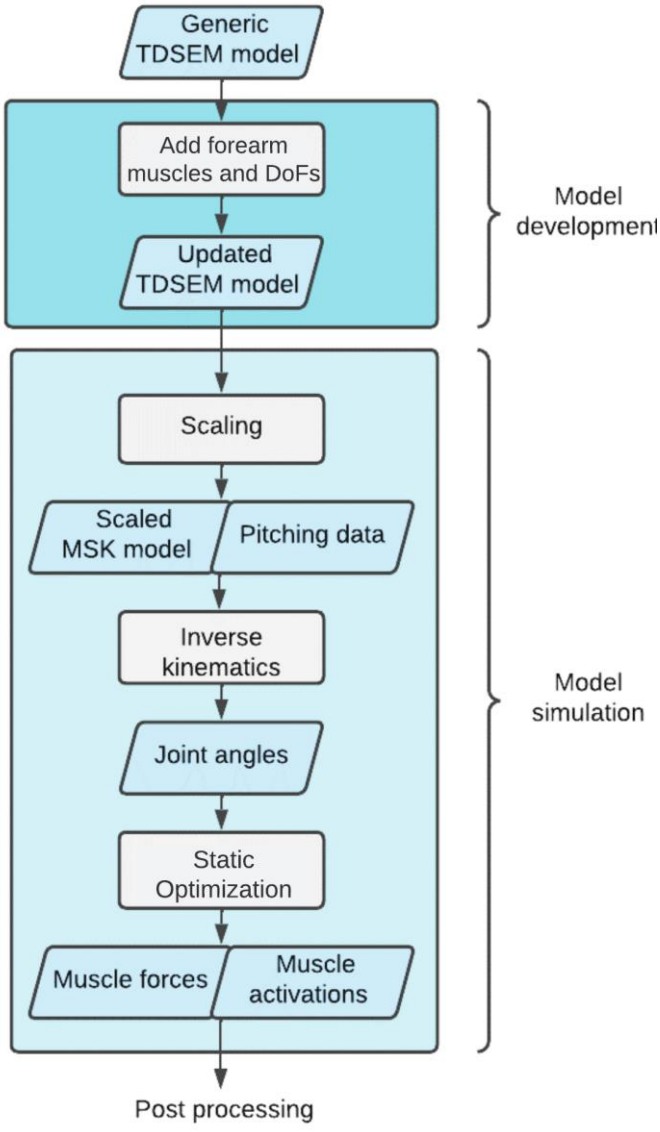

Fig.9. A flowchart of all the model development and simulation steps.

2.5. Post-processing

2.5.1. Muscle moments

With the results of the SO, the individual muscle forces (F^i_{muscle}), and the determined muscle moment arms (r^i) (Fig.7), the moments of each individual muscle around the varus-valgus axis were calculated (M^i_{muscle}). The force generated by each muscle was multiplied by its varus-valgus moment arm (Eq.1).

$$M^i_{muscle}(t) = F^i_{muscle}(t) * r^i(t) \quad (1)$$

The direction of each individual muscle moment is based on its moment arm. In this model the BIC, BRD, ECRB, ECRL, ECU and EDC generate internal valgus torques ($M_{muscle,valgus}$) and the TRI, BRA, PRO, FCR, FCU and FDS generate internal varus torque ($M_{muscle,varus}$) (Fig.7). Summation of these twelve individual muscle moments generates a resultant internal moment acting on the elbow (M_{muscle}), either negative (valgus) or positive (varus) (Eq.2, Fig.10).

$$M_{muscle}(t) = \sum_{i=1}^{12} M^i_{muscle}(t) \quad (2)$$

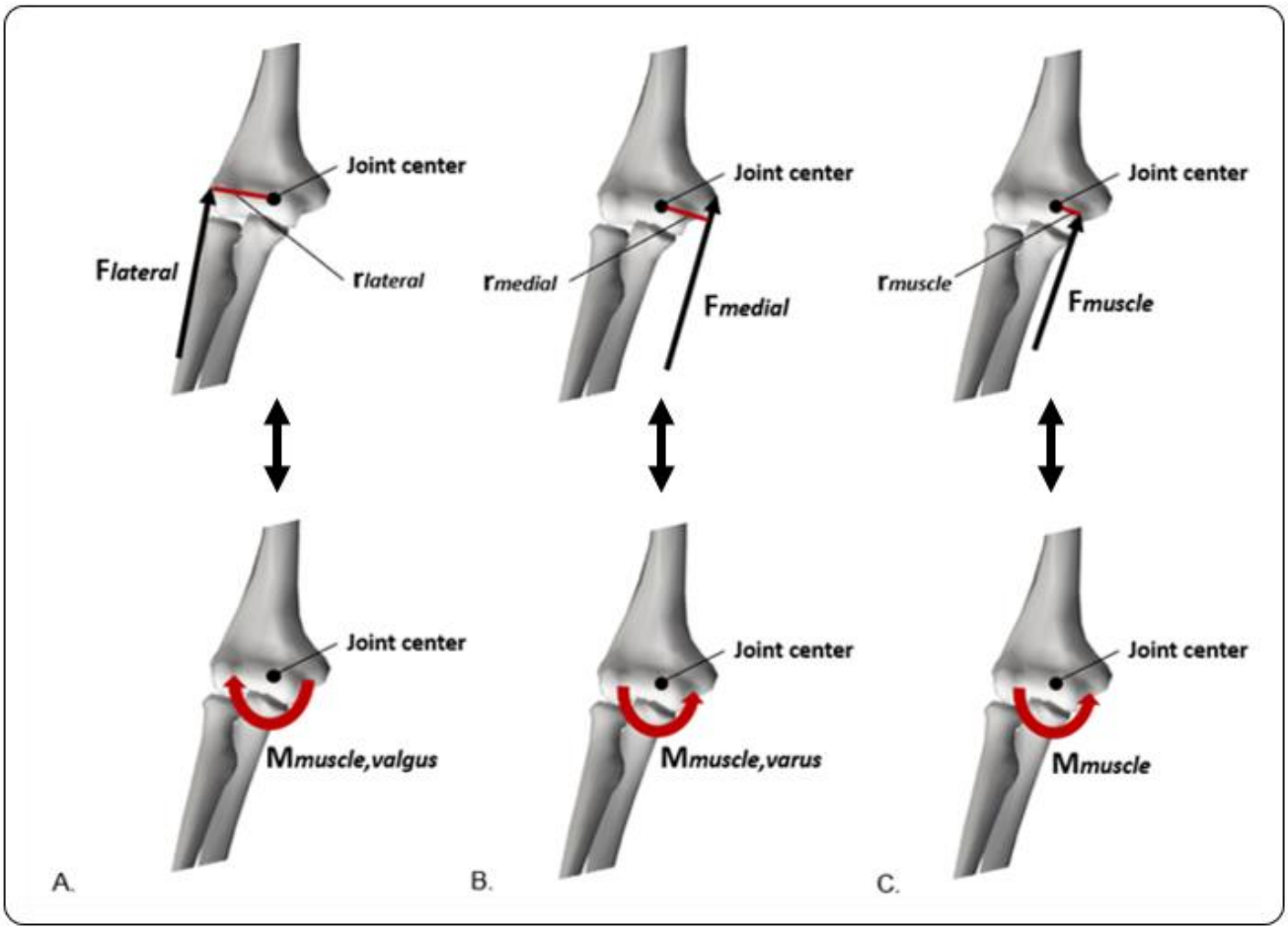

Fig. 10. Freebody diagrams of the elbow joint showing: A. The resultant internal valgus moment ($M_{muscle,valgus}$) generated by the BIC, BRD, ECRB, ECRL, ECU and EDC. B. The resultant internal varus moment generated by the TRI, BRA, PRO, FCR, FCU and FDS ($M_{muscle,varus}$). C. The summation of all individual muscle moments generating a resultant internal moment (M_{muscle}) (direction unknown).

2.5.2. UCL torque load

To calculate the UCL torque load, a torque balance around the varus-valgus axis was used (Fig.2.). Based on the results of previous studies (Morrey et al., 1981; Lin et al., 2007, Seiber et al., 2009; Udall et al., 2009; Buffi et al., 2015; Van Trigt, 2021) it can be assumed that the external valgus torque exposed to the elbow (M_{valgus}) is countered by an internal varus torque distributed among ligamentous structures (M_{UCL}), the osseous articulation (M_{art}) and elbow muscles (M_{muscle}) (Eq.3, Fig.11).

$$M_{valgus}(t) = M_{UCL}(t) + M_{muscle}(t) + M_{art}(t) \quad (3)$$

Rearranging gives:

$$M_{UCL}(t) = M_{valgus}(t) - \left(M_{muscle}(t) + M_{art}(t)\right) \quad (4)$$

SO simulations were used to determine M_{valgus}. SO uses inverse dynamics to find generalized forces/moments which satisfy the classical equation of motion. The motion of the model is defined by its generalized positions (s) and their derivatives; velocities (v) and accelerations (a). The generalized forces causing the model's motion (M_{valgus}) are equal and opposite to the summation of the model's mass matrix ($M_{mass}(s)$) times the accelerations (a), the vector of Coriolis and centrifugal forces ($C(s,v)$), and the vector of gravitational forces ($G(s)$) (Eq. 5). The generalized forces calculated using this equation are composed of the resultant muscle moment and the moment caused by the reserve actuator (T) placed at the model's varus-valgus DoF (Eq.6).

$$M_{valgus}(t) = M_{mass}(s)a + C(s,v) + G(s) \quad (5)$$

$$M_{valgus}(t) = M_{muscle}(t) + T(t) \quad (6)$$

Substituting equation 6 in 4 equation gives:

$$M_{UCL}(t) = M_{muscle}(t) + T(t) - \left(M_{muscle}(t) + M_{art}(t)\right) \quad (7)$$

$$= T(t) - M_{art}(t) \quad (8)$$

M_{art} is caused by an offset from the joint center to the center of pressure (CoP) for the contact between the humerus and the forearm during valgus motion. This offset causes the joint compression force (F_{joint}) to generated a moment around the CoP (M_{art}). M_{art} is calculated by multiplying F_{joint} by its moment arm (r_{joint}), which presents the offset from the joint center to the CoP (Eq. 9).

$$M_{art}(t) = F_{joint}(t) * r_{joint}(t) \quad (9)$$

F_{joint} is determined using the joint reaction analysis tool in OpenSim 4.1. This tool calculates the joint forces and moments transferred between consecutive bodies as a result of all loads acting on the model. The component of the resultant force vector parallel to the longitudinal axis of the radius was defined to be F_{joint}. Duggan et al. (2011) defined the CoP in the elbow under a valgus load as the contact area between the radius and the humerus. In this study, r_{joint} was defined to be half the length of the vector from the joint center to the lateral edge of the radius, following the paper of Buffi et al. (2015).

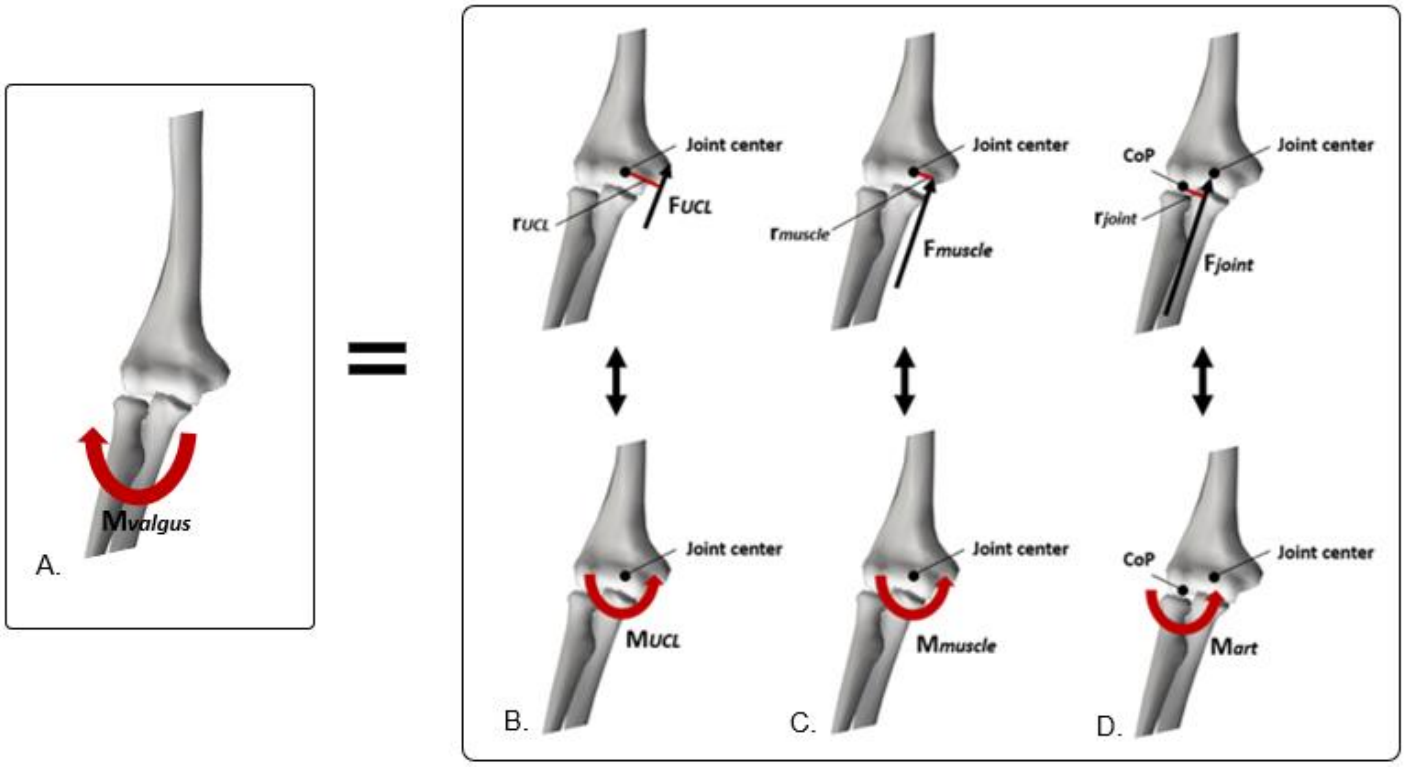

Fig.11. Freebody diagrams of the internal varus moments countering the external valgus moment (Eq.3). A. External valgus moment. B. Definition of the force and moment generated by the UCL. C. Definition of the resultant muscle force and moment. D. Definition of the moment generated by the osseous articulation.

3. Results

Muscle-driven simulations for ten baseball pitches were generated. Inverse kinematics accuracy for each trial was within two cm RMSE concerning experimental marker locations. The kinematic data of the pitches were synchronized at the instant of the maximal external valgus moment (MEV) and cut at the moment of foot contact and ball release. The average maximum external valgus torque placed on the elbow over the ten pitches (M_{valgus}) was determined to be 82.3 Nm (Fig. 13). The average duration of the cocking-acceleration phase was 0.408 s.

3.1. Muscle forces and muscle moments

At MEV all muscles were active and able to generate force during the wrist-included simulations. The biggest and smallest force was generated by the TRI (617.0 N) and the ECRL/ECRB (0.014 N) respectively, at MEV. Over the whole motion, the TRI also generated the biggest force with the peak force of 824.3 N occurring before MEV. During the wrist-excluded simulations the ECU, ECRL and ECRB were not able to generate force during the simulations. The BRA, BRD, EDC and FDS generated substantial smaller forces than during the wrist-included simulations. Reversely, the BIC, TRI, PRO and FCR generated substantial larger forces than during the wrist-included simulations. The biggest force at MEV was again generated by the TRI, although a bit lower (550.7 N). The biggest force over the whole motion, was also generated by the TRI, now occurring after MEV (1225 N). The FDS generated the smallest forces at MEV (1.4 N).

When looking at the individual muscle moments (Fig. 15), the FDS had the biggest contribution to the total internal varus moment at MEV (4 Nm) during the wrist included simulations. The second biggest contributors to the total internal varus moment are the TRI with a moment of 3.5 Nm at MEV. The moments generated by ECRL, ECRB, ECU and SUP are negligibly small. Except for the PRO, FCU and EDC, all muscles generate their peak moments after the MEV. The EDC is the biggest contributor to the total internal valgus moment with a moment of -2.9 Nm at MEV. Other muscles producing internal valgus moments were the BIC and the BRD. Together they generated a resultant internal valgus moment of -5.7 Nm at MEV. The TRI, BRA, PRO, FCR, FCU and FDS generated a resultant internal varus moment of 14.3 Nm at MEV. The resultant of all individual muscle moments has a peak varus moment right after MEV (11.6 Nm). At MEV the resultant of the individual muscle moments has a value of 8.5 N.

When looking at the individual muscle moments during the wrist excluded simulations, the FCR had the biggest contribution to the total internal varus moment with a peak of 8.2 Nm just before MEV. The second biggest contributors to the total internal varus moment are still the TRI with a peak of 7.8 Nm just after MEV. Besides the fact that the ECU, ECRL and ECRB were not able to generate any moments, the moments generated by FDS and SUP are negligibly small. Except for the PRO and FCR, all muscles generate their peak moments after the MEV. The EDC is again the biggest contributor to the total internal valgus moment with a moment of -2.4 Nm at MEV. Other muscles producing internal valgus moments were the BIC and the BRD. Together they generated a resultant internal valgus moment of -5.1 Nm. The TRI, BRA, PRO, FCR, FCU and FDS generated a resultant internal varus moment of 13.3 Nm. The resultant of all individual muscle moments has a peak varus moment right before MEV (15.6 Nm). At MEV the resultant of the individual muscle moments has a value of 8.1 Nm. Overall, the patterns that emerged in individual muscle moments in wrist-included simulations were comparable to wrist-excluded simulations, but differ in magnitude (Fig. 15).

3.2. UCL torque load

M_{valgus} was determined to be 82.3 Nm at MEV (Fig. 13). During the wrist-included simulations, M_{muscle} had a value of 8.5 Nm at MEV (Fig 16). F_{joint} had a value of 1636 N at MEV. Based on anthropometric measurements of the model, r_{joint} is determined to be 25 mm, resulting in M_{art} of 48.2 (Eq. 9). The moment the UCL has to withstand (M_{UCL}) was determined to be 25.6 Nm. This moment is 56.7 Nm (69%) smaller than $M_{valgus.}$ M_{valgus} gets countered for 10% by M_{muscle}, for 59% by M_{art} and for 31% by M_{UCL}. During the wrist-excluded simulations, M_{muscle} has a peak varus moment right before MEV (15.6 Nm). At MEV, M_{muscle} has a value of 8.1 Nm (Fig. 16). F_{joint} had a value of 1035 N at MEV, resulting in M_{art} of 34.7 Nm at MEV (Eq. 9). M_{UCL} was calculated to be 39.4 Nm. This moment is 42.9 Nm (52%) smaller than $M_{valgus.}$ M_{valgus} gets countered for 10% by M_{muscle}, for 42% by M_{art} and for 48% by M_{UCL} (Fig. 12).

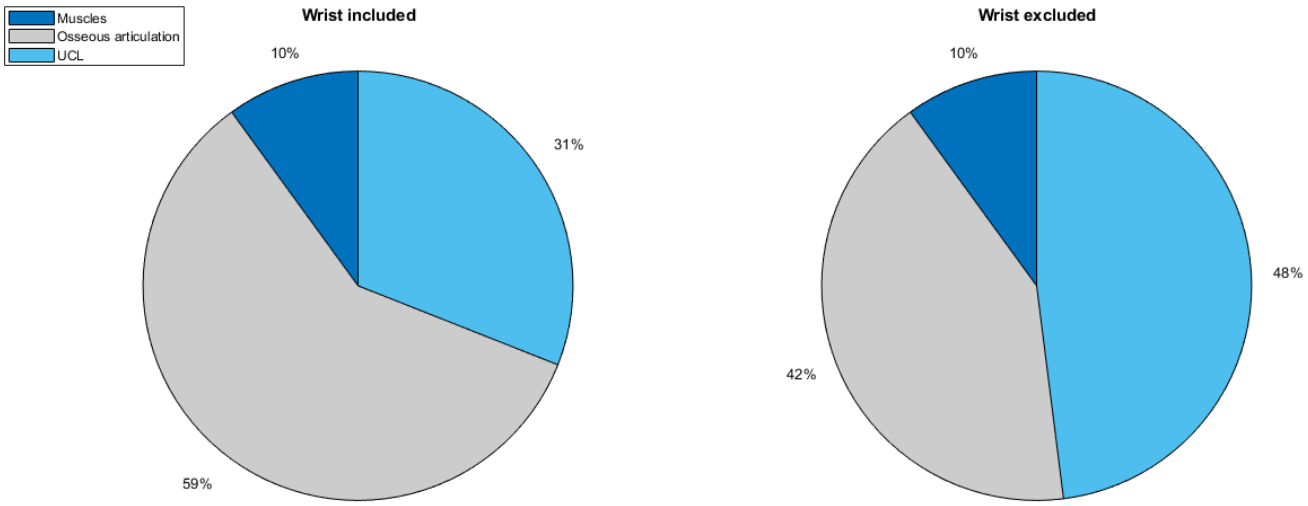

Fig.12. Distribution of the external valgus moment placed on the elbow over the elbow stabilizers; the muscles, osseous articulation and UCL for the wrist-included simulations (left) and the wrist-excluded simulations (right).

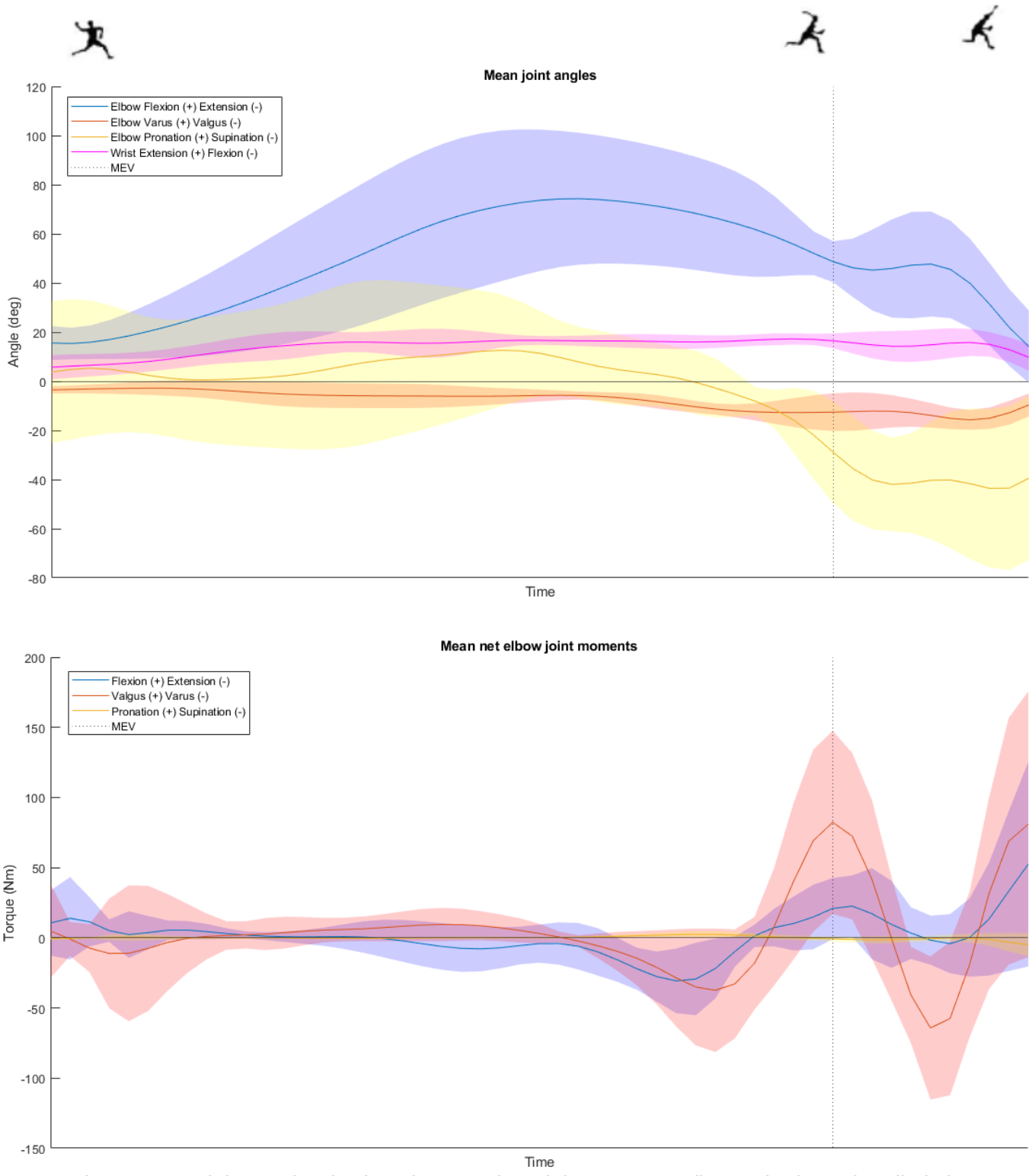

Fig.13. Mean joint angles (top) and external net joint moments (bottom) +/- SD for all pitchers.

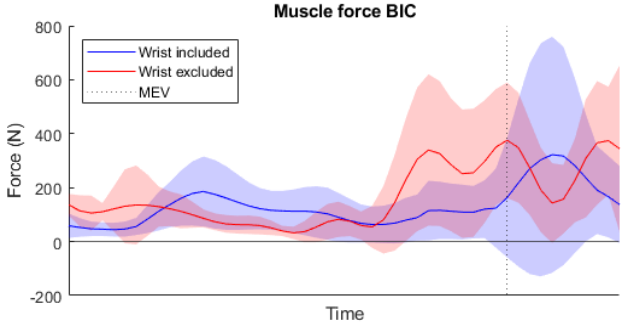
Muscle force BIC
Wrist included
Wrist excluded
MEV
Force (N)
Time


Muscle force TRI
Wrist included
Wrist excluded
MEV
Force (N)
Time

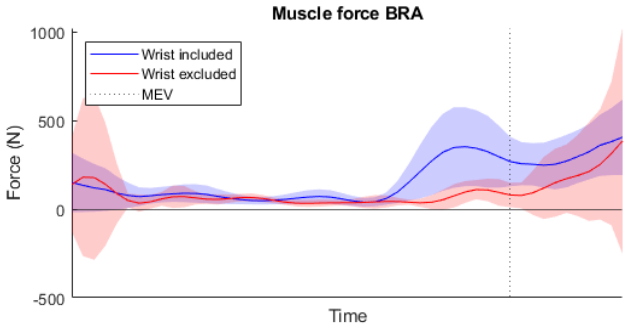
Muscle force BRA
Wrist included
Wrist excluded
MEV
Force (N)
Time

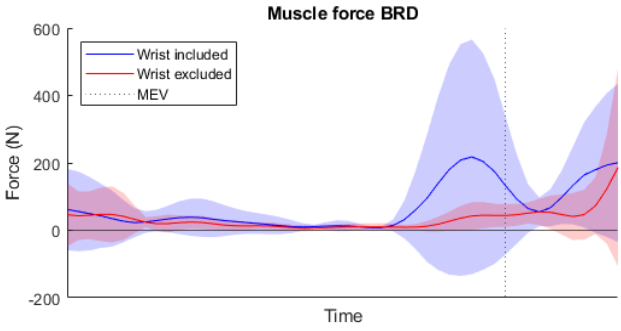
Muscle force BRD
Wrist included
Wrist excluded
MEV
Force (N)
Time

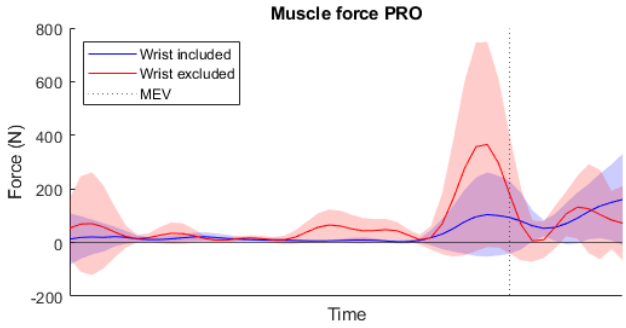
Muscle force PRO
Wrist included
Wrist excluded
MEV
Force (N)
Time

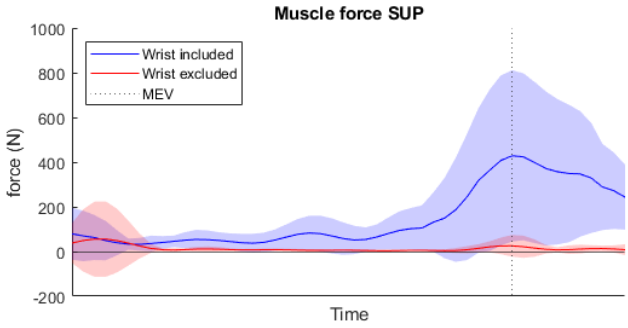
Muscle force SUP
Wrist included
Wrist excluded
MEV
force (N)
Time

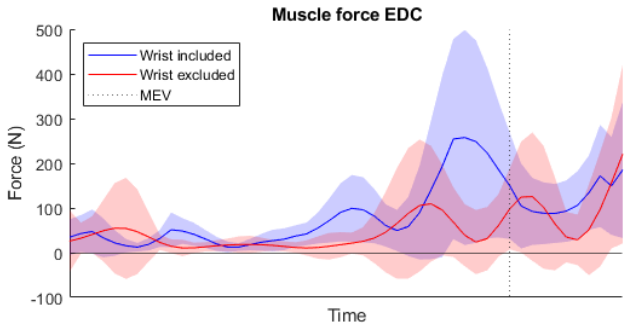
Muscle force EDC
Wrist included
Wrist excluded
MEV
Force (N)
Time

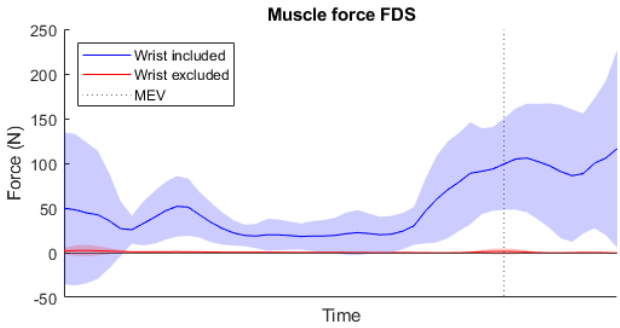
Muscle force FDS
Wrist included
Wrist excluded
MEV
Force (N)
Time

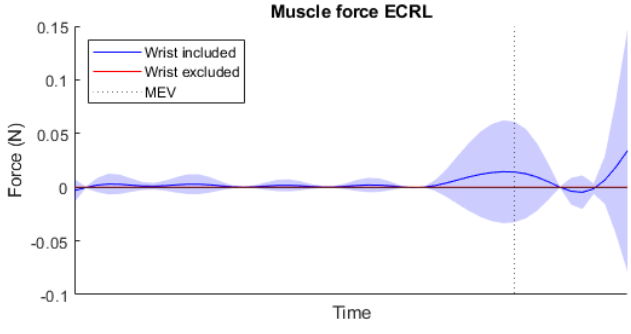
Muscle force ECRL
Wrist included
Wrist excluded
MEV
Force (N)
Time

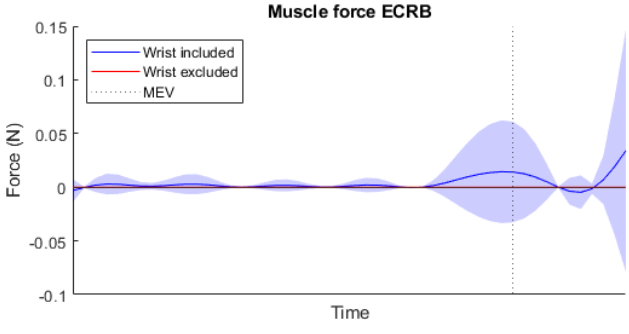
Muscle force ECRB
Wrist included
Wrist excluded
MEV
Force (N)
Time

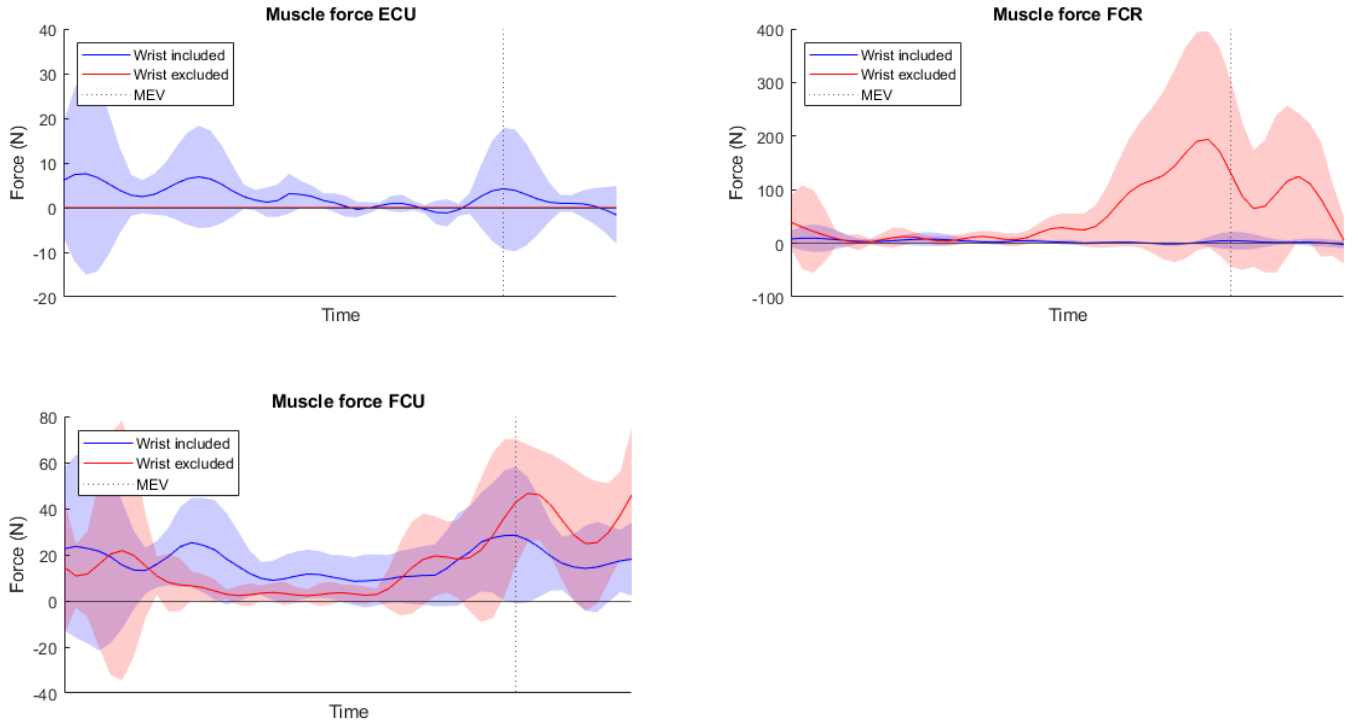

Fig.14. Mean muscle force +/- SD of all elbow muscles for all pitchers.

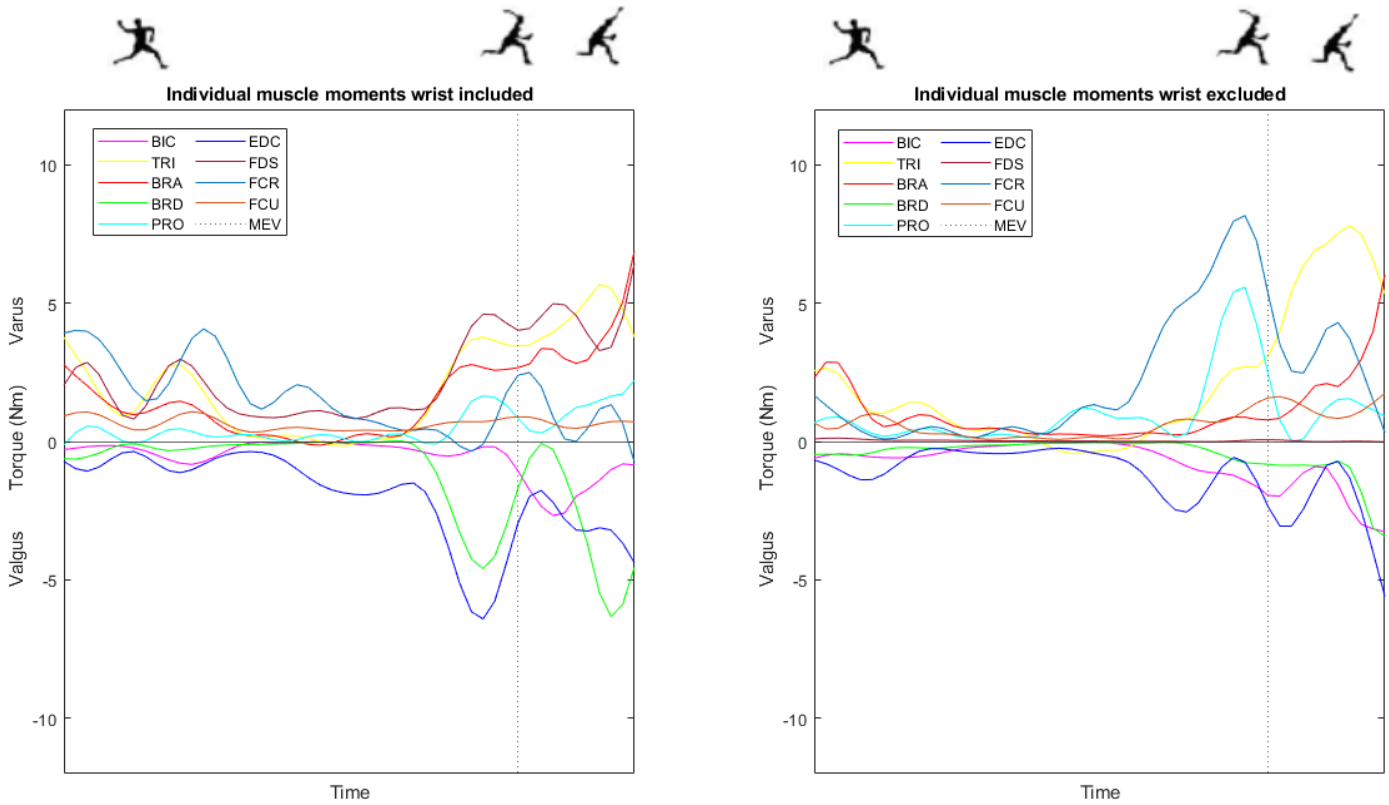

Fig.15. Left: Internal varus-valgus moments generated by the individual muscles during the wrist-included simulations. Right: Internal varus-valgus moments generated by the individual muscles during the wrist-excluded simulations. The ECU, ECRL, ECRB and SUP are not included in the figures, since they generated neglectable small varus-valgus moments during both simulations.

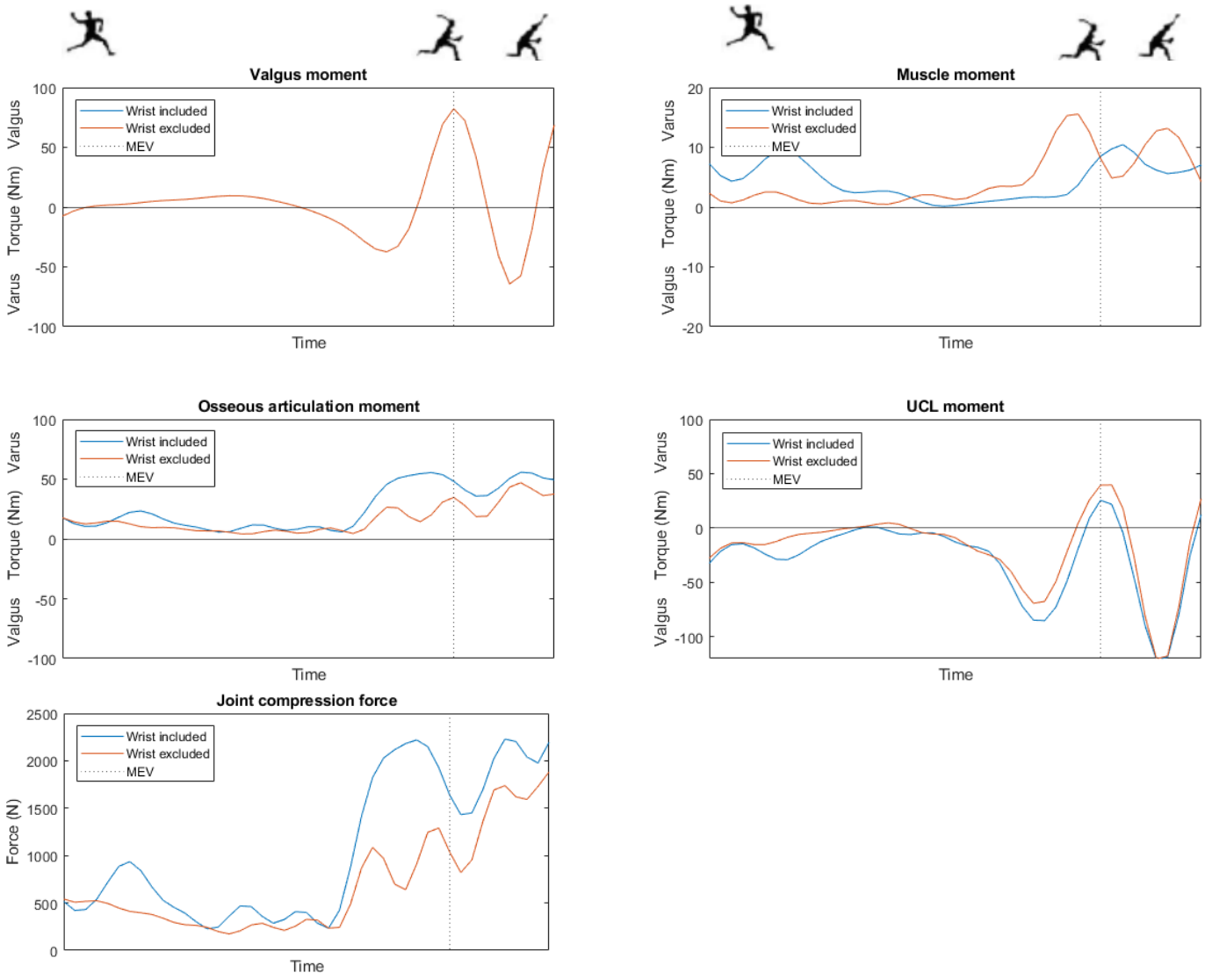

Fig.16. Overview of the external valgus moments placed on the elbow and the internal varus moments caused by the joint compression force, the muscle forces and the UCL.

4. Discussion

The purpose of this study was to identify the muscles capable of (un)loading the UCL during baseball pitching. A previously developed OpenSim MSK model of the upper extremity was extended by adding forearm muscles. Using this model, the arm cocking and acceleration phases of ten pitches were simulated. The model was able to produce pitching kinematics and dynamics similar to pitching kinematics and dynamics published in previous studies (Zheng et al., 2004). The high variation in the pitching kinematics and dynamics between the pitchers can be explained by the fact that a heterogenous group of pitchers with different levels of play and age participated in this study. To investigate the individual muscles muscle moments at the instant of external peak valgus moment, the instant of external peak valgus moment during each pitch was firstly determined using inverse dynamics. Secondly, individual muscle force and activation patterns were determined using SO. Finally, the individual muscle moments, the elbow joint compression force and the torque load on the UCL were computed in some post-processing steps.

During the wrist-included simulations all muscles were able to generate force. The TRI generated the biggest force at MEV. The TRI is able to produce big forces due to its large volume and physiological cross-sectional area (An et al.,1981). In addition, the elbow is flexing throughout the whole motion, but goes into extension halfway through (Fig.13). This causes elbow flexors to contract eccentrically and elbow extensors to contract concentrically. Muscles are able to generate larger forces during eccentric contractions than concentric contraction, causing the TRI to generate such high forces (Zajac, 1989). The ECRL/ECRB generated the smallest force at MEV, followed by the ECU. The small force generated by these muscles can be explained by its function. The main function of the ECRL/ECRB is wrist abduction and of the ECU wrist adduction. The wrist in the model is not able to perform these motions, therefore the muscles do not have to produces forces to cause these motions.

In this model the BIC, BRD and EDC generate internal valgus moments and the TRI, BRA, PRO, FCR, FCU and FDS generate internal varus moments. The FDS was the biggest contributor to the total internal varus moment. The big contribution of the FDS to the total internal varus moment just before MEV can be explained by the fact the FDS has a relatively large varus-valgus moment arm. The FDS is active to keep the wrist in its slightly extended position. To do so, the FDS is contracting eccentrically, just like the TRI. The EDC is the biggest contributor to the total internal valgus moment. The EDC produced high forces during the pitch causing wrist extension. All muscles were capable of generating muscle moments, although the moments generated by the ECRL, ECRB, ECU and SUP were negligible small due to small forces generated by the ECRL, ECRB and ECU and the small varus-valgus moment arm of the SUP.

The M_{valgus} was distributed over the UCL (31%), the muscles (10%) and the osseous articulation (59%), resulting in a varus moment for the UCL to resist of 25.6 Nm. This value is below the moment the UCL can resists (30 Nm). This means that the UCL, the muscles and the osseous articulation together are able to counter external valgus loads in a manner that is not harmful for the UCL. In addition, the osseous articulation can be defined as main elbow stabilizer during pitching motions. This is in contrast with previous studies reporting the UCL as primary stabilizer of the elbow (Morrey et al., 1981; Lee & Rosenwasser, 1999).

A few differences between the results of the wrist-included and wrist-excluded simulations were found. Unlike during the wrist-included simulations, during the wrist-excluded simulations the ECU, ECRL and ECRB did not generate any force throughout the pitching motion. This can be explained by the function of these muscles. These muscles are primary wrist abductors and adductors, but additionally they can cause wrist extension. Since the motion of the wrist is locked in this model, these muscles do not have to generate force. In addition, the BRA, BRD, EDC and FDS generated substantial smaller forces during the wrist-excluded simulations. The small force generated by the FDS and EDC can also be explained by their function. The main functions of these muscles are flexion and extension of the fingers and wrist respectively. Since the wrist and fingers are locked during the wrist-excluded simulations, the muscles do not have to produce any force to cause these motions. The small force generated by the BRA and BRD can be explained by dynamic coupling. Muscles spanning the wrist joint not only act to accelerate the joint it spans, but also other joints, like the elbow (Zajac, 1993; Zajac and Gordon, 1989). Excluding wrist motion altered the force generated by the wrist spanning muscles and this may result in altered acceleration of the elbow joint, resulting in less need for the BRA and BRD to generate force to cause elbow flexion. In addition, the BIC, TRI, PRO and FCR generated substantial larger forces, possibly for the same reason. The FCR was the biggest contributor to the total internal varus moment during the wrist-excluded simulations. The force generated by the FCR together with its relatively large varus-valgus moment arm, results in a large internal varus moment. The FDS was the smallest contributor to the total internal varus, since it generated small forces, due to the fact that it did not have to generate force to cause wrist motion. Overall, the pattern of the resultant muscle moments showed quite some differences, with higher internal varus moments occurring before and after MEV during the wrist-excluded simulations than during the wrist-included simulations. However, at MEV the resultant moments were quite similar (Fig. 16). During the wrist-excluded simulations the total valgus moment placed the elbow was distributed over the UCL (48%), the muscles (10%) and the osseous articulation (42%), resulting in a varus moment for the UCL to resist of 39.4 Nm. This value exceeds the moment the UCL can resists (30 Nm). This means that the UCL, the muscles and the osseous articulation together are not able to counter external valgus loads in a manner that is not harmful for the UCL, when the wrist stays in neutral position during pitching.

The muscle activation patterns for both simulations are in good agreement with previous reported EMG data. The flexor pronator mass, PRO, TRI, BIC, extensor supinator mass and ANC showed moderate activity at MER (Van Trigt et al., 2021). Results of the simulations are consistent with this EMG data, since all these muscles were active during the pitch. Results of the individual muscle moment are partly in line with the cadaveric studies investigating the role of elbow muscles in reducing tension on the UCL. The FCU, FCR, FDS and PRO were reported to be able to lessen the tension on the UCL (Davidson et al., 1995; Lin et al., 2007, Seiber et al., 2009; Udall et al., 2009). These muscles had indeed a substantial contribution to the total internal varus moment and these findings reinforce the results of the cadaveric studies. The SUP, BRD, ECRB, ECRL, EDC and ECU were reported to induce a valgus motion of the elbow (Lin et al., 2007; Seiber et al., 2009). The BRD and EDC indeed induced valgus motion of the elbow by generating internal valgus moments. However, the SUP, ECRB, ECRL and ECU were not be able to generate a substantial internal valgus moment during pitching motions. Additionally, co-contraction of the elbow flexor and extensor muscles were reported to be possible contributors in counteracting the external valgus torque by increasing the joint compression force of the elbow joint (Morrey et al., 1991; Seiber et al., 2009; Ferreira et al., 2010; Van Trigt et al., 2021). These findings are consistent with the results of the simulations, since the TRI, BIC, BRA and BRD were active simultaneously.

Results of the simulations show the distribution of the external valgus torque over the UCL, the elbow muscles and the osseous articulation. The osseous articulation can be identified as main stabilizer of the elbow. The results show that motion of the wrist has influence on M_{art}, and lowers the UCL toque. A bigger M_{art} was found during wrist-included simulations than wrist-excluded simulations. This is probably caused by co-contraction of the BRA and BRD, since higher activations of these muscle were found during the wrist-included simulations than during the wrist-excluded simulations. Understanding how wrist motion contribute to co-contraction of the elbow muscle could help inform more effective training during pitching, protecting the UCL from injury.

This study comprises several limitations. First of all, to predict the muscle forces and activations SO was used. The SO algorithm computes the active force along a muscle's tendon, assuming a rigid tendon and neglecting the contributions of muscle-excitation- and tendon-dynamics. OpenSim also contains another optimization technique; computed muscle control (CMC). The contribution of the passive muscle force to the steady-state muscle force are included by CMC, which results in estimation of larger muscle forces and activations (Roelker et al., 2016). Several studies have compared the results of SO and CMC (Wesseling et al., 2014; Rankin et al., 2016; Lin et al., 2011; Mokhtarzadeh et al., 2014). Some reported that SO is the best optimization technique for estimating muscle function in human locomotion due to its robustness and computational efficiency (Lin et al., 2011; Mokhtarzadeh et al., 2014). However, joint torques determined from CMC were more accurate compared with those from SO (Roelker et al., 2016). Although the experimental data are rather controversial, and there is no general agreement about what technique to use, it is important to keep in mind which technique is used to determine muscle forces and activations when comparing results.

Secondly, anatomical parameters of the model were obtained from multiple sources, instead of single source. According to Goislard De Monsabert et al. (2017), this can bias predicted muscle force. Use of a model with a single source data set will likely improve muscle force predictions. However, there is currently no data-set available including all the required anatomical parameters for this model.

Thirdly, the muscle geometry of the model is validated by comparing the muscle moment arms of the model with muscle moment arms taken from literature. Values of moment arms for EFE and PS from literature were derived from both cadaveric measurements and MSK model calculations. It should be noted that there are large discrepancies among the available cadaver specimen sources and considerable variation in measurement techniques. Some of the moment arm data provided only two- to three-moment arm measurements across an entire range of motion, resulting in a very limited means of comparison to our model. For validation of the moment arms during EVV only one source is used. Currently, there is very limited data on varus-valgus moments available. A more complete anatomical data set of the elbow muscle including muscle moments arms is required to make the development and validation of MSK easier in the future.

Fourthly, the model used in this study is a generic model linearly scaled to match the participant's anthropometry. This method disregards the variation in musculoskeletal geometry and tissue properties between individuals. In contrast, subject-specific models can mimic participants' musculoskeletal anatomy derived from medical imaging. This can lead to differences in joint centers, body segment inertia and muscle moment arms between participants and eventually to more accurate predictions of individual muscle moments (Akhundov et al., 2022). It may be beneficial to use a subject-specific model when investigating baseball kinematics and/or dynamics in the future, since muscle geometry and properties may differ in baseball players from an average 50th percentile male.

Lastly, the influence of different wrist flexion angles on muscle forces and the UCL load during pitching was not under investigation. Only wrist angles with an average value of ten and zero degrees were investigated. In addition, motion at the finger joints was not included in this study. Motion of these joints could influence the force patterns from muscles. Further research is needed to fully understand the influence of wrist and finger motion on UCL load. In this way, more effective training can be developed in order to protect the UCL from injury during pitching.

5. Conclusion

Understanding how the individual elbow muscles contribute to the UCL load can lead to effective training of specific muscles and may alter the UCL load during pitching, protecting the UCL from injury. This study aimed to identify the muscles capable of (un)loading the UCL during baseball pitching. Results show that the BIC, BRD and EDC are able to load the UCL by generating internal valgus torques. Reversely, the TRI, BRA, PRO, FCR, FCU and FDS are able to unload the UCL by generating internal varus torques. The FDS is the biggest contributor to the total internal varus moment and the EDC is the biggest contributor to the total internal valgus moment. The external valgus moment placed on the elbow was countered for 10% by the elbow muscles, 59% by the osseous articulation and 31% by the UCL, resulting in a moment for the UCL to resist of 25.6 Nm. Based on these results, the osseous articulation can be identified as the main stabilizer of the elbow. In addition, a bigger contribution of the osseous articulation was found during wrist motion included simulations than during wrist motion excluded simulations. Baseball coaches and pitchers should pay attention to keep the wrist in an extended position during pitching at least till after the beginning of the arm acceleration phase. In this way the contribution of the osseous articulation to counter the external valgus torque will be bigger than when the wrist stays in neutral position. Additionally, squeezing the ball with the fingers during pitching could possibly higher the force generated by the FDS, resulting in a bigger contribution of this muscle to counter the external valgus torque. Further research should focus on investigating the influence of wrist and finger motion on UCL load and focus more on muscles/motions influencing the joint compression since the osseous articulation is identified as the main stabilizer of the elbow during pitching. In this way, more effective training can be developed to protect the UCL from injury during pitching.

Acknowledgements

This study could not have been carried out without the help of my supervisors Frans van der Helm and Bart van Trigt. I would like to thank Bart van Trigt in particular for his daily guidance and advice. Furthermore, I would like to thank Ajay Seth for answering all my questions about OpenSim. Additionally, I want to thank my fellow students who were always available for discussions and ideas. Last but not least, I want to thank my family and friends who had to listen to my struggles throughout this journey and kept me motivated.

Bibliography

Ahmad, C. S., Lee, T. Q., & ElAttrache, N. S. (2003). Biomechanical Evaluation of a New Ulnar Collateral Ligament Reconstruction Technique with Interference Screw Fixation. *The American Journal of Sports Medicine*, *31*(3), 332–337. https://doi.org/10.1177/03635465030310030201

Akhundov, R., Saxby, D. J., Diamond, L. E., Edwards, S., Clausen, P., Dooley, K., Blyton, S., & Snodgrass, S. J. (2022). Is subject-specific musculoskeletal modelling worth the extra effort or is generic modelling worth the shortcut? *PLOS ONE*, *17*(1), e0262936. https://doi.org/10.1371/journal.pone.0262936

An, K., Hui, F., Morrey, B., Linscheid, R., & Chao, E. (1981). Muscles across the elbow joint: A biomechanical analysis. *Journal of Biomechanics*, *14*(10), 659–669. https://doi.org/10.1016/0021-9290(81)90048-8

Anz, A. W., Bushnell, B. D., Griffin, L. P., Noonan, T. J., Torry, M. R., & Hawkins, R. J. (2010). Correlation of Torque and Elbow Injury in Professional Baseball Pitchers. *The American Journal of Sports Medicine*, *38*(7), 1368–1374. https://doi.org/10.1177/0363546510363402

Buffi, J. H., Werner, K., Kepple, T., & Murray, W. M. (2014). Computing Muscle, Ligament, and Osseous Contributions to the Elbow Varus Moment During Baseball Pitching. *Annals of Biomedical Engineering, 43(2*), 404–415. https://doi.org/10.1007/s10439-014-1144-z

Conte S, Camp CL, Dines JS. (2016) Injury trends in Major League Baseball over 18 seasons: 1998-2015. *Am J Orthop (Belle Mead NJ)*.45(3):116–123

Correa, T. A., Baker, R., Kerr Graham, H., & Pandy, M. G. (2011). Accuracy of generic musculoskeletal models in predicting the functional roles of muscles in human gait. *Journal of Biomechanics*, *44*(11), 2096–2105. https://doi.org/10.1016/j.jbiomech.2011.05.023

Davidson, P. A., Pink, M., Perry, J., & Jobe, F. W. (1995). Functional Anatomy of the Flexor Pronator Muscle Group in Relation to the Medial Collateral Ligament of the Elbow. *The American Journal of Sports Medicine*, *23*(2), 245–250. https://doi.org/10.1177/036354659502300220

De Vet, J. (2021). *Opensim upper-extremity modelling: subject-specific scaling- and validation tools* (Master's thesis). Retrieved from http://resolver.tudelft.nl/uuid:8ccea623-8b7e-4539-a395-21614f42d70b

Delp, S. L., Anderson, F. C., Arnold, A. S., Loan, P., Habib, A., John, C. T., Guendelman, E., & Thelen, D. G. (2007). OpenSim: Open-Source Software to Create and Analyze Dynamic Simulations of Movement. *IEEE Transactions on Biomedical Engineering*, *54*(11), 1940–1950. https://doi.org/10.1109/tbme.2007.901024

Duggan, J. P., Osadebe, U. C., Alexander, J. W., Noble, P. C., & Lintner, D. M. (2011). The impact of ulnar collateral ligament tear and reconstruction on contact pressures in the lateral compartment of the elbow. *Journal of Shoulder and Elbow Surgery*, *20*(2), 226–233. https://doi.org/10.1016/j.jse.2010.09.011

Ferreira LM, King GJ, Johnson JA. Development of an active elbow flexion simulator to evaluate joint kinematics with the humerus in the horizontal position. *J Biomech.* 2010;43(11):2114e2119.

Fleisig, G. S., Andrews, J. R., Dillman, C. J., and Escamilla, R. F. (1995). Kinetics of baseball pitching with implications about injury mechanisms. Am. J. Sports Med. 23, 233–239. doi: 10.1177/036354659502300218

Frost, D. M., Cronin, J., & Newton, R. U. (2010). A Biomechanical Evaluation of Resistance. *Sports Medicine*, *40*(4), 303–326. https://doi.org/10.2165/11319420-000000000-00000

Gonzalez, R. V., Hutchins, E. L., Barr, R. E., & Abraham, L. D. (1996). Development and Evaluation of a Musculoskeletal Model of the Elbow Joint Complex. *Journal of Biomechanical Engineering*, *118*(1), 32–40. https://doi.org/10.1115/1.2795943

Lee ML, Rosenwasser MP. (1999) Chronic elbow instability. *Orthop Clin North Am*. 30(1):81-89

Leland, D. P., Conte, S., Flynn, N., Conte, N., Crenshaw, K., Wilk, K. E., & Camp, C. L. (2019). Prevalence of Medial Ulnar Collateral Ligament Surgery in 6135 Current Professional Baseball Players: A 2018 Update. *Orthopaedic journal of sports medicine, 7(9)*, 2325967119871442. https://doi.org/10.1177/2325967119871442

Lin, F., Kohli, N., Perlmutter, S., Lim, D., Nuber, G. W., & Makhsous, M. (2007). Muscle contribution to elbow joint valgus stability. *Journal of Shoulder and Elbow Surgery*, *16*(6), 795–802. https://doi.org/10.1016/j.jse.2007.03.024

Lin, Y. C., Dorn, T. W., Schache, A. G., & Pandy, M. G. (2011). Comparison of different methods for estimating muscle forces in human movement. *Proceedings of the Institution of Mechanical Engineers, Part H: Journal of Engineering in Medicine*, *226*(2), 103–112. https://doi.org/10.1177/0954411911429401

Lu, T. W., & O'Connor, J. (1999). Bone position estimation from skin marker co-ordinates using global optimisation with joint constraints. *Journal of Biomechanics, 32(2),* 129–134. https://doi.org/10.1016/s0021-9290(98)00158-4

Maniar, N., Cole, M. H., Bryant, A. L., & Opar, D. A. (2022b). Muscle Force Contributions to Anterior Cruciate Ligament Loading. *Sports Medicine*. https://doi.org/10.1007/s40279-022-01674-3

McGraw, M. A., Kremchek, T. E., Hooks, T. R., & Papangelou, C. (2012). Biomechanical Evaluation of the Docking Plus Ulnar Collateral Ligament Reconstruction Technique Compared With the Docking Technique. *The American Journal of Sports Medicine*, *41*(2), 313–320. https://doi.org/10.1177/0363546512466375

Md, C. A. S., Ms, A. A. T., & Ahmad, C. J. (2017). Understanding Tommy John Surgery and How to Avoid It: A Guide for Young Baseball Players (1ste editie). Lead Player LLC.

Meldau, J. E., Srivastava, K., Okoroha, K. R., Ahmad, C. S., Moutzouros, V., & Makhni, E. C. (2020). Cost analysis of Tommy John surgery for Major League Baseball teams. *Journal of Shoulder and Elbow Surgery, 29*(1), 121–125. https://doi.org/10.1016/j.jse.2019.07.019

Mirakhorlo, M., Visser, J. M. A., Goislard De Monsabert, B. A. A. X., Van der Helm, F. C. T., Maas, H., & Veeger, H. E. J. (2016). Anatomical parameters for musculoskeletal modeling of the hand and wrist. *International Biomechanics*, *3*(1), 40–49. https://doi.org/10.1080/23335432.2016.1191373

Mokhtarzadeh, H., Perraton, L., Fok, L., Muñoz, M. A., Clark, R., Pivonka, P., & Bryant, A. L. (2014). A comparison of optimisation methods and knee joint degrees of freedom on muscle force predictions during single-leg hop landings. *Journal of Biomechanics*, *47*(12), 2863–2868. https://doi.org/10.1016/j.jbiomech.2014.07.027

Morray, B. F., Tanaka, S., & An, K. N. (1991). Valgus Stability of the Elbow. *Clinical Orthopaedics and Related Research*, *265*(NA;), 187-195. https://doi.org/10.1097/00003086-199104000-00021

Morrey, B. F., & An, K. N. (1983). Articular and ligamentous contributions to the
O'Connell, R. S., & Field, L. D. (2020). Handheld Osteotomes Facilitate Arthroscopic Treatment of Elbow Valgus Extension Overload. *Arthroscopy Techniques*, *9*(3), e387–e391. https://doi.org/10.1016/j.eats.2019.11.004

Ramsay, J. W., Hunter, B. V., & Gonzalez, R. V. (2009). Muscle moment arm and normalized moment contributions as reference data for musculoskeletal elbow and wrist joint models. *Journal of Biomechanics, 42(4),* 463–473. https://doi.org/10.1016/j.jbiomech.2008.11.035

Rankin, J. W., Rubenson, J., & Hutchinson, J. R. (2016). Inferring muscle functional roles of the ostrich pelvic limb during walking and running using computer optimization. *Journal of The Royal Society Interface*, *13*(118), 20160035. https://doi.org/10.1098/rsif.2016.0035

Roelker, Sarah & Caruthers, Elena & Baker, Rachel & Pelz, Nicholas & Chaudhari, Ajit & Siston, Robert. (2016). Static Optimization vs. Computed Muscle Control Characterizations of Neuromuscular Control: Clinically Meaningful Differences?.

Schellenberg, F., Oberhofer, K., Taylor, W. R., & Lorenzetti, S. (2015). Review of Modelling Techniques for In Vivo Muscle Force Estimation in the Lower Extremities during Strength Training. *Computational and Mathematical Methods in Medicine*, 2015, 1–12. https://doi.org/10.1155/2015/483921

Seiber, K., Gupta, R., McGarry, M. H., Safran, M. R., & Lee, T. Q. (2009). The role of the elbow musculature, forearm rotation, and elbow flexion in elbow stability: An in vitro study. *Journal of Shoulder and Elbow Surgery*, *18*(2), 260–268. https://doi.org/10.1016/j.jse.2008.08.004

Stodden, D. F., Fleisig, G. S., McLean, S. P., Lyman, S. L., & Andrews, J. R. (2001). Relationship of Pelvis and Upper Torso Kinematics to Pitched Baseball Velocity. *Journal of Applied Biomechanics*, *17*(2), 164–172. https://doi.org/10.1123/jab.17.2.164

Thelen, D. G., & Anderson, F. C. (2006). Using computed muscle control to generate forward dynamic simulations of human walking from experimental data. *Journal of Biomechanics*, *39*(6), 1107–1115. https://doi.org/10.1016/j.jbiomech.2005.02.010

Thelen, D. G., Anderson, F. C., & Delp, S. L. (2003). Generating dynamic simulations of movement using computed muscle control. *Journal of Biomechanics*, *36*(3), 321–328. https://doi.org/10.1016/s0021-9290(02)00432-3

Udall, J. H., Fitzpatrick, M. J., McGarry, M. H., Leba, T. B., & Lee, T. Q. (2009). Effects of flexor-pronator muscle loading on valgus stability of the elbow with an intact, stretched, and resected medial ulnar collateral ligament. *Journal of Shoulder and Elbow Surgery*, *18*(5), 773–778. https://doi.org/10.1016/j.jse.2009.03.008

Valente, G., Crimi, G., Vanella, N., Schileo, E., & Taddei, F. (2017). nmsBuilder : Freeware to create subject-specific musculoskeletal models for OpenSim. *Computer Methods and Programs in Biomedicine*, 152, 85–92. https://doi.org/10.1016/j.cmpb.2017.09.012

Van Trigt, B., Galjee, E., Hoozemans, M. J. M., Van der Helm, F. C. T., & Veeger, D. H. E. J. (2021). Establishing the Role of Elbow Muscles by Evaluating Muscle Activation and Co-contraction Levels at Maximal External Rotation in Fastball Pitching. *Frontiers in Sports and Active Living, 3*. https://doi.org/10.3389/fspor.2021.698592

Wesseling, M., Derikx, L. C., De Groote, F., Bartels, W., Meyer, C., Verdonschot, N., & Jonkers, I. (2014). Muscle optimization techniques impact the magnitude of calculated hip joint contact forces. *Journal of Orthopaedic Research*, *33*(3), 430–438. https://doi.org/10.1002/jor.22769

Zajac, F. E. (1989). Muscle and tendon: properties, models, scaling, and application to biomechanics and motor control. *Crit. Rev. Biomed. Eng*. 17:359–411

Zajac, F. E. (1993). Muscle coordination of movement: A perspective. *Journal of Biomechanics*, *26*, 109–124. https://doi.org/10.1016/0021-9290(93)90083-q

Zajac, F. E., & Gordon, M. E. (1989). Determining Muscles Force and Action in Multi-Articular Movement. *Exercise and Sport Sciences Reviews*, *16*, 187-230. https://doi.org/10.1249/00003677-198900170-00009

Zheng, N., Fleisig, G. S., Barrentine, S., & Andrews, J. R. (2004). Biomechanics of Pitching. In G. K. Hung & J. M. Pallis (Eds.), *Biomedical engineering principles in sports* (pp. 209–256). Boston, MA: Springer US. doi:10.1007/978-1-4419-8887-4_9

Appendix A: Muscles TDSEM

Muscle Group	Number of muscle-elements	Source
Anconeus	5	De Vet
Biceps Longus	3	De Vet
Brachialis	7	De Vet
Brachioradialis	3	De Vet
Coracobrachialis	3	De Vet
Deltoid Clavicula	4	De Vet
Deltoid Scapula	11	De Vet
Extensor Carpi Radialis	2	Mirakhorlo et al.
Extensor Carpi Ulnaris	2	Mirakhorlo et al.
Extensor Digitorum Communis	4	Mirakhorlo et al.
Flexor Carpi Radialis	1	Mirakhorlo et al.
Flexor Carpi Ulnaris	1	Mirakhorlo et al.
Flexor Digitorum Superficialis	4	Mirakhorlo et al.
Infraspinatus	6	De Vet
Latissimus Dorsi	6	De Vet
Levator Scapulae	2	De Vet
Lumbrical	4	Mirakhorlo et al.
Opponens Digitorum Minimi	1	Mirakhorlo et al.
Opponens Pollicis	6	Mirakhorlo et al.
Palmar Interosseus	3	Mirakhorlo et al.
Pectoralis Major Clacivula	2	De Vet
Pectoralis Major Sternocostal	6	De Vet
Pectoralis Minor	4	De Vet
Pronator Quadratus	3	De Vet
Pronator Teres	2	De Vet
Romboid	5	De Vet
Serratus Anterior	12	De Vet
Subscapularis	11	De Vet
Supinator	1	De Vet
Supraspinatus	4	De Vet
Teres Major	4	De Vet
Teres Minor	3	De Vet
Trapezus Clavicula	2	De Vet
Trapezus Scapula	12	De Vet
Triceps Lateralis	5	De Vet
Triceps Longus	4	De Vet
Triceps Medialis	5	De Vet

Table 1. Overview of all muscles included into the model.

Appendix B: Initial validation results

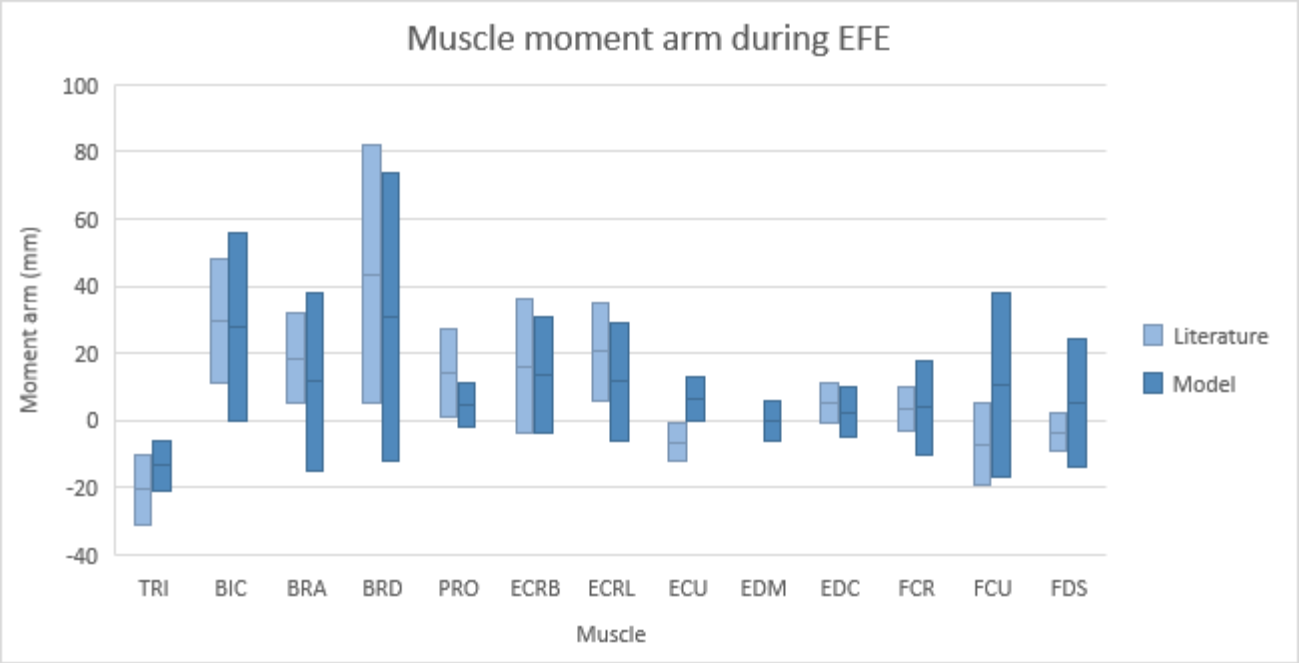

Fig.1. Comparison of literature moment arm range and model moment arm range during EFE. Positive and negative values correspond to elbow flexion and extension, respectively.

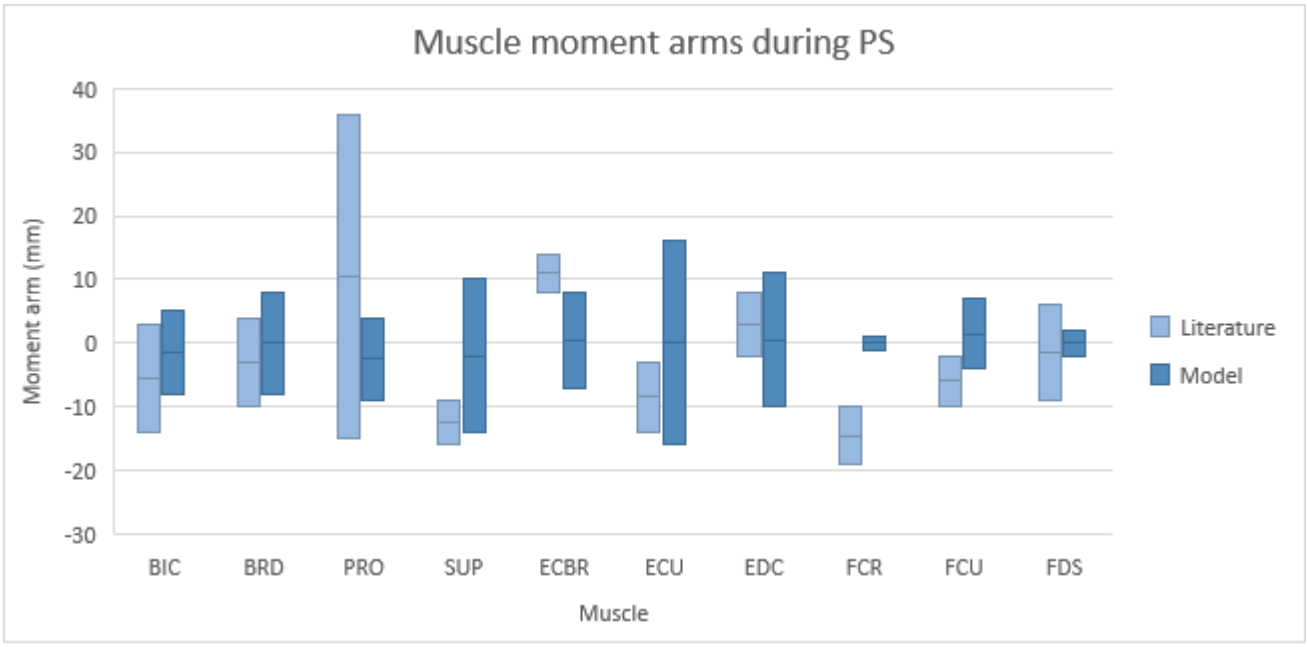

Fig.2. Comparison of literature moment arm range and model moment arm range during PS. Positive and negative values correspond to forearm pronation and supination, respectively.

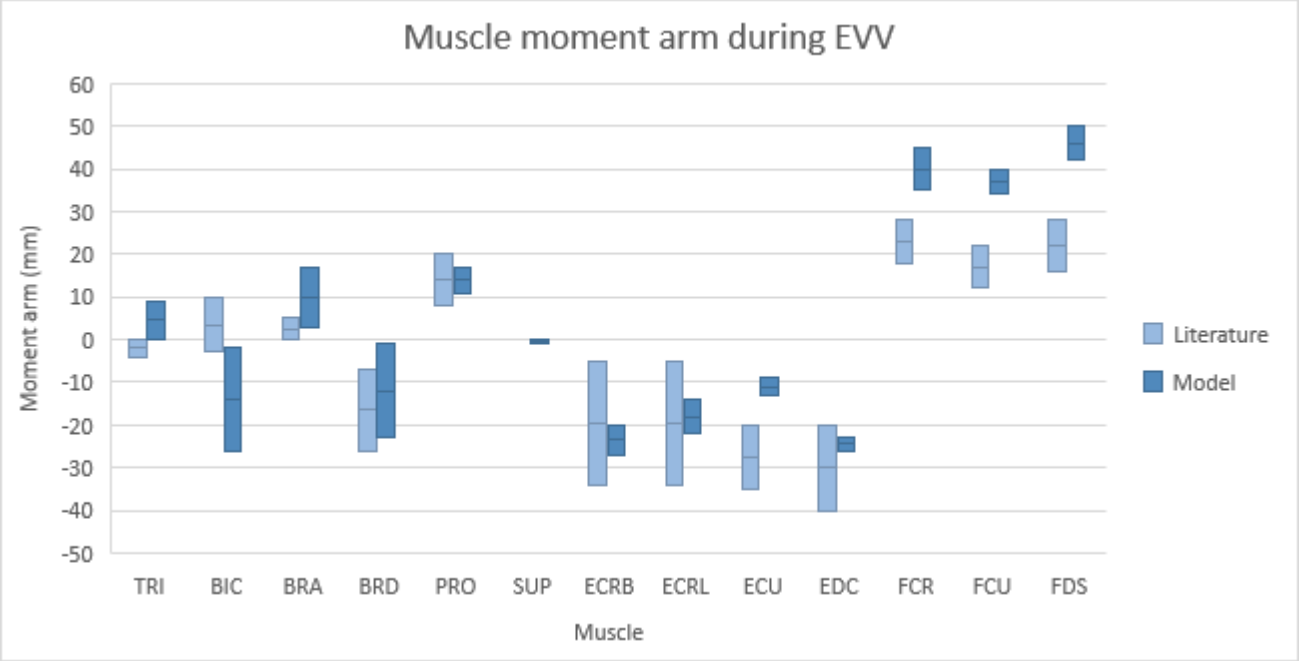

Fig.3. Comparison of literature moment arm range and model moment arm range during PS. Positive and negative values correspond to elbow varus and valgus, respectively.

Appendix C: Marker placement

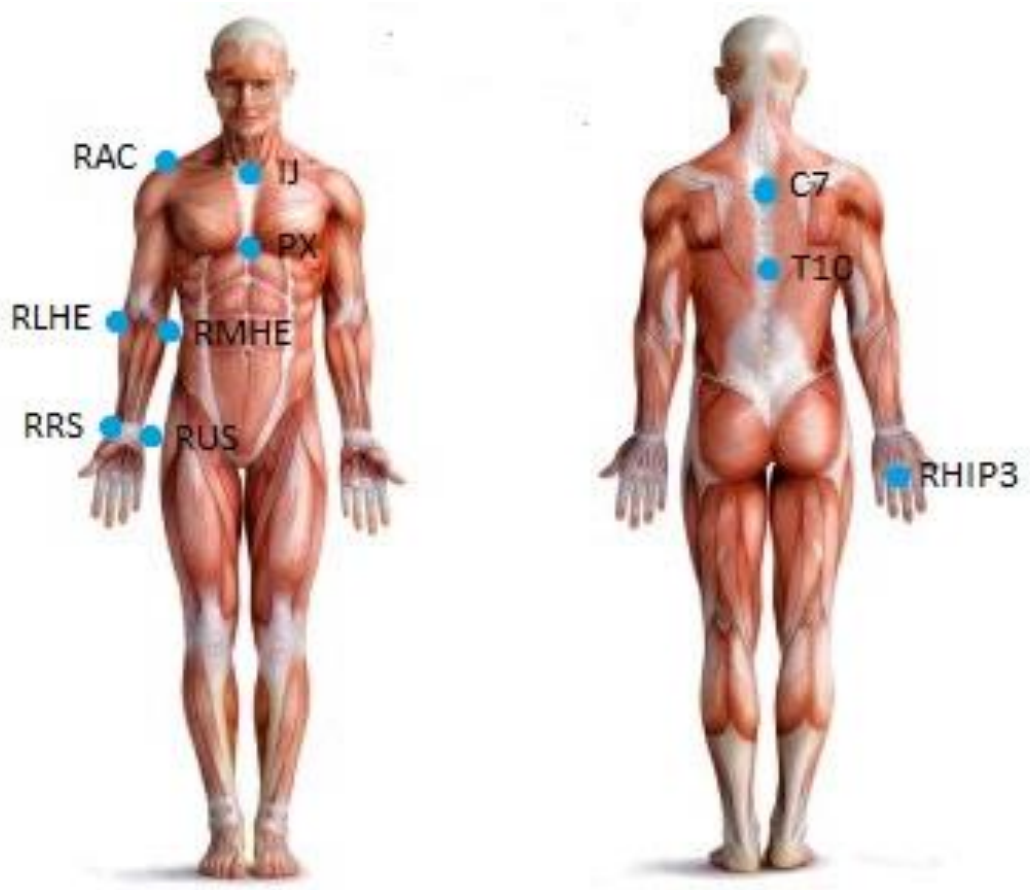

Fig. 1. Posterior and anterior view of the marker placement on each subject corresponding to anatomical landmarks; Incisura Jugularis (IJ), Processus Xiphoideus (PX), Cervical Vertebrae 7 (C7), Thoracic Vertebrae 10 (T10), Right Acromioclavicular Joint (RAC), Right Epicondylus Medialis (RMHE), Right Epicondylus Lateralis (RLHE), Right Wrist Head of Ulna (RUS), Right Styloid Processes of Radius (RRS), Right Hand Interphalangealis proximal III (RHIP3).